www.sciencemag.org/content/356/6333/62/suppl/DC1

Supplementary Material for

High-performance vitrimers from commodity thermoplastics through dioxaborolane metathesis

Max Röttger, Trystan Domenech, Rob van der Weegen, Antoine Breuillac, Renaud Nicolaÿ,* Ludwik Leibler*

*Corresponding author. Email: renaud.nicolay@espci.fr (R.N.); ludwik.leibler@espci.fr (L.L.)

Published 7 April 2017, *Science* **356**, 62 (2017)
DOI: 10.1126/science.aah5281

This PDF file includes:

Materials and General Characterization Methods

Chemicals and solvents

Chemicals were purchased from Sigma Aldrich, Alfa Aesar, TCI, Acros Organics and Fischer. Unless otherwise noted, reagents were used without further purification. Poly(methyl methacrylate)s (M_n = 92 kg/mol and M_w = 129 kg/mol) used for mechanical testing were provided by Arkema. High-density polyethylene (HDPE, melt index 2.2 g/10 min at 190 °C for 2.16 kg) and poly(methyl methacrylate) (PMMA, M_w~120 000 g/mol) homopolymer used for comparison in adhesion tests, were purchased from Sigma-Aldrich. Solvents (including deuterated solvents) were used and stored under inert atmosphere over fresh and dried molecular sieves 3Å for at least 72 hours to achieve maximum dryness (*31*). Before use and addition of compounds for exchange reactions on dioxaborolanes, glassware was oven-dried, heated with a heat gun while being purged with dry argon (< 0.5 ppm H_2O). Methyl methacrylate (MMA) and styrene (S) were purified by passing through a column filled with basic alumina to remove inhibitors or antioxidants. 2,2'-Azobis(2-methylpropionitrile) (AIBN) was recrystallized from methanol. Diols were dried over magnesium sulfate ($MgSO_4$) and filtered before use.

Gel permeation chromatography (GPC)

GPC was performed on a Viscotek GPCmax/VE2001 connected to a Triple detection array (TDA 305) from Malvern. Obtained raw data were treated with the respective standard homopolymer calibration curve (PMMA and polystyrene (PS)).

Solution and solid phase Fourier-transform infrared (FT-IR) spectroscopy

FT-IR spectroscopy was performed out on a Tensor 37 spectrometer from Bruker. Solution phase absorbance spectra were recorded in chloroform using a liquid cell with KBr windows and a 1 mm path length (Teflon spacer). Solid state spectra of small molecules, functionalized polyethylene and poly(methylmethacrylate) materials were recorded in attenuated total reflectance (ATR) mode and converted to absorbance spectra.

Nuclear magnetic resonance (NMR) spectroscopy measurements

^{1}H-NMR and ^{13}C-NMR spectroscopy measurements were performed in oven dried NMR tubes on a Bruker Ultra Shield machine at 400 MHz and 100 MHz, respectively. If not stated otherwise, samples of 10 mg were analyzed and the obtained data were internally referenced to the standard shift of the respective solvent.

Mass spectrometry measurements

Mass spectrometry measurements were performed on a Trace-GC Ultra gas chromatograph coupled to an ITQ900 (Thermo Scientific), and performed by electronic impact ionization in positive ion mode. Specific isotopic pattern of organoboron compounds were observed.

Samples preparation by compression molding

HDPE specimens were pressed for characterization via compression molding at 150 °C for 10 minutes. Poly(methyl methacrylate) samples were pressed at 150 °C for 10 minutes and polystyrene samples for 5 minutes at 150 °C. Samples were generated using

disc shape (diameter of 25 mm, thickness of 1.5 mm), bar shape (length of 35 mm, width of 5 mm, thickness of 1.5 mm) and film shape (thickness of 1.5 mm) frames. Dumbell-shaped tensile specimens (ISO 527-2 type 5B) were prepared from pressed films using a punch cutter.

Samples preparation by injection molding

Materials were injection molded on a DSM Xplore micro 10 cm^3 injection molding machine into disc or dog-bone shape. Samples (3.0 g) were injected at 200 °C under 12 bar into the preheated mold (180 °C) during a total of 15 seconds before cooling down to 45 °C by using a water circuit (ca. 3 minutes).

Synthesis and Characterization

1. Thermogravimetric and solubility studies of stability of PMMA polymer and networks containing pending diols and dioxaborolane

The syntheses of PMMA polymers and networks studied in this Section are described below in Section 4 p9-p13.

Thermogravimetric analysis (TGA)

TGA was performed on a TG 209 F1 Libra from Netzsch under nitrogen flow. The samples were kept at 25 °C for 5 minutes, ramped to a desired temperature in a period of 5 minutes and then kept at constant temperature for a specified time.

TGA experiments were used to gain insight into high-temperature stability of PMMA based polymers and vitrimers. Samples of PMMA with pending diols (**10**) and pending dioxaborolanes (**11**) were subjected to elevated temperatures under a protective flow of nitrogen and afterwards swollen or dissolved in THF to determine the insoluble fraction (Table S1). PMMA-diol **10** shows a high insoluble fraction (98.5% and 97.3%) when treated at 200 °C for 10 or 5 minutes, respectively, while PMMA-boronic ester (PMMA-BE) **11** remains fully soluble. The TGA and subsequent solubility experiments indicate that side-reactions take place at elevated temperatures in PMMA-diol **10** resulting in the formation of a cross-linked insoluble network, even for short times. A possible explanation for this is the transesterification of the diol fragments onto the ester groups of the methacrylate repeating units, with the liberation of methanol.

Further experiments were performed on PMMA V5 and PMMA-diol V5 (a network similar to PMMA V5 but with pending diols instead of pending dioxaborolanes). After the TGA experiment, the networks were allowed to swell or dissolve in THF in the presence of excess 1,2-propanediol to transesterify dioxaborolane bonds. In the case of PMMA V5, the network is fully soluble after dioxaborolane diolysis, while for the corresponding network based on pending diols (PMMA-diol V5) an insoluble gel is observed. These results indicate that side-reactions occurred in the networks based on diol/dioxaborolane exchange, which lead to the formation of permanent non exchangeable cross-links. Similar to the linear PMMA polymers with pending diol functionalities, transesterification of the diol fragments onto the ester moieties of the methacrylate repeating units would result in the formation of a permanent non dynamic network.

2. Synthesis and characterization of model dioxaborolanes

General procedure for the synthesis and characterization of dioxaborolanes

The diol (1.0 eq), the boronic acid (1.05 eq) and 0.1 vol% of water were mixed in diethyl ether (Et_2O) (2 mL/1 mmol boronic acid) at room temperature and stirred until complete dissolution of all compounds. $MgSO_4$ (3.0 eq) was added stepwise and the mixture was stirred at room temperature for 5 hours, filtered and concentrated under reduced pressure. The suspension was immersed in heptane, stirred for 30 minutes at room temperature, filtered and the liquid phase was concentrated under reduced pressure. The resulting oil was distilled at 150 °C under high vacuum to yield the target compounds with very high purity as colorless oils (65-80%) (Fig. S2). The purified boronic esters were transferred directly to dried and purged Schlenk flasks and kept under protective atmosphere.

4-Methyl-2-phenyl-1,3,2-dioxaborolane (**B_1-D_1**): ^{1}H-NMR (400 MHz, $CDCl_3$): δ 7.84 p.p.m. (d, J = 5.6 Hz, 2H), 7.52-7.38 (m, 3H), 4.78-4.68 (m, 1H), 4.64 (dd, J = 1.2 Hz, 8.8 Hz, 1H), 3.90 (dd, J = 1.6 Hz, 8.8 Hz, 1H), 1.43 (d, J = 6.4 Hz, 3H). ^{13}C-NMR (100 MHz, $CDCl_3$): δ 134.7, 131.5, 127.9, 73.7, 72.4, 21.8. Carbon adjacent to boron not detected. Purity of **B_1-D_1**: GC (FID) no impurities detected. ^{1}H-NMR: no diol detected.

4-Ethyl-2-phenyl-1,3,2-dioxaborolane (**B_1-D_2**): ^{1}H-NMR (400 MHz, $CDCl_3$): δ 7.84 p.p.m. (d, J = 6.4 Hz, 2H), 7.51-7.48 (m, 3H), 4.55 (m, 1H), 4.43 (dd, J = 8.8 Hz, 1.2 Hz 1H), 3.98 (dd, J = 2.0 Hz, 8.8 Hz, 1H), 1.82-1.63 (m, 2H), 1.04 (t, J = 7.6 Hz, 3H). ^{13}C-NMR (100 MHz, $CDCl_3$): δ 134.9, 131.4, 127.8, 78.6, 70.8, 29.0, 9.0. Carbon adjacent to boron not detected. Purity of **B_1-D_2**: GC (FID) no impurities detected. ^{1}H-NMR: no diol detected.

4-Methyl-2-(3,5-dimethylphenyl)-1,3,2-dioxaborolane (**B_2-D_1**): ^{1}H-NMR (400 MHz, $CDCl_3$): δ 7.46 p.p.m. (s, 2H), 7.13 (s, 1H), 4.73 (m, 1H), 4.46 (dd, J = 8.8 Hz, 1.2 Hz, 1H), 3.90 (dd, J = 8.8 Hz, 1.2 Hz, 1H), 2.34 (s, 6H), 1.43 (d, J = 6.0 Hz, 3H). ^{13}C-NMR (100 MHz, $CDCl_3$): δ 137.2, 133.2, 132.5, 73.72, 72.5, 21.8, 21.2. Carbon adjacent to boron not detected. Purity of **B_2-D_1**: GC (FID) no impurities detected. ^{1}H-NMR: no diol detected. MS (m/z): [M] calcd for $C_{11}H_{15}BO_2$, 190.1165; found, 190.07.

4-Ethyl-2-(3,5-dimethylphenyl)-1,3,2-dioxaborolane (**B_2-D_2**): ^{1}H-NMR (400 MHz, $CDCl_3$): δ 7.45 p.p.m. (s, 2H), 7.12 (s, 1H), 4.56-4.94 (m, 1H), 4.42 (dd, J = 0.8 Hz, 8.8 Hz, 1H), 3.96 (dd, J = 2.0 Hz, 8.8 Hz, 1H), 2.35 (s, 6H), 1.80-1.62 (m, 2H), 1.02 (t, J = 7.6 Hz, 3H). ^{13}C-NMR (100 MHz, $CDCl_3$): δ 137.4, 133.2, 132.9, 78.5, 70.7, 28.8, 20.9, 8.7. Carbon adjacent to boron not detected.

3. Kinetic study of dioxaborolanes metathesis

Determination of the detection limit of 1,2 butanediol (**D_2**) in ^{1}H-NMR spectroscopy and dioxaborolane purity

The detection limit of free diol compounds in ^{1}H-NMR spectroscopic analysis was determined by decreasing the concentration of 1,2-butanediol (**D_2**) in dried $CDCl_3$. Styrene was used as an internal standard in a concentration of 25.0 mM and added to the deuterated solvent before use and drying over molecular sieves. A stock solution of **D_2** at a concentration of 25.5 mM was generated and further diluted with the deuterated solvent. Six solutions were analyzed in total. For a concentration of 0.1 mM, the signals of **D_2** cannot be detected anymore, with the exception of the CH_3-signal at 0.98 ppm. With the detection limit of 0.1 mM, the maximum free diol content in the synthesized dioxaborolanes **B_1-D_2** and **B_2-D_1** was calculated with equation S1 by analyzing highly concentrated boronic ester solutions (Table S2).

Equation S1
Determination of the maximum diol content in boronic esters **B_1-D_2** and **B_2-D_1**

$$[diol]_{max}(\%) = \frac{[diol]_{max}}{\langle [diol]_{max} + [boronic\ ester] \rangle}$$

$$= \frac{0.1\ \text{mM}}{\langle 0.1\ \text{mM} + 1000\ \text{mM} \rangle} = 0.01$$

Gas chromatography (GC) and exchange reactions

GC was conducted on a Shimadzu gas chromatograph GC-2014 equipped with a Zebron-5HT "inferno" column and using helium as carrier gas. Injection was done manually by injecting samples of 1 µL using a 10 µL syringe from Hamilton (gastight 1701). Before running the analysis, the entire set-up was pre-heated to 350 °C and kept at constant carrier gas flow of 5 mL/min and split ratio of 2.0 for at least 30 minutes. Samples were analyzed with a flame ionization detector (FID). External calibration curves with characteristic response factors for each boronic ester were generated. To this end, 0.1 mmol of the respective dioxaborolane was added to 1 g of the respective solvent and 100, 50 and 10 µL of this solution was further diluted with 0.1 mL of the solvent and injected into the GC apparatus (Fig. S4). Internal calibration was performed by the addition of dried tetradecane to the reaction medium before drying and storage over molecular sieves under protective atmosphere. Reactants were mixed in oven dried and argon-purged Schlenk flask. The reaction mixtures were kept under inert atmosphere at all times. The following GC method was used for calibrations and analysis of the exchange reactions: $T_{injection/detector}$ = 350 °C, T_{column} = 120 °C, T_{ramp} = 30 °C/min, carrier gas flow 5.0 mL/min and split ratio = 2.0. Samples were taken with cleaned, dried and argon-purged needles and either injected into the GC apparatus directly (exchange in tetrahydrofuran (THF) or added to a small volume of dried dichloromethane (DCM) (dried, under argon) to dilute each sample mixture before injection (bulk). The results (Figs. S2-S7, Table S2) suggest the occurrence of a direct exchange (metathesis) between

boronic esters instead of the previously described diol/boronic ester transesterification or hydrolysis based exchange of boronic esters (17, *32-39*).

Equation S2

$$\frac{d[B_1D_1]}{dt} = -\frac{d[B_1D_2]}{dt} = k[B_1D_2][B_2D_1] - k[B_1D_1][B_2D_2]$$

With $[B_1D_2] = [B_2D_1]$ and $[B_1D_1] = [B_2D_2]$

4. Synthesis and characterization of dioxaborolane vitrimers from vinylic monomers

a. Synthesis of dioxaborolane vitrimers from vinylic monomers

Synthesis and characterization of vinylic monomers

4-(2,2-Dimethyl-1,3-dioxolan-4-yl)butan-1-ol **1**: 1,2,6-Hexanetriol (25 g, 186 mmol) was dissolved in acetone (340 mL) in the presence of $MgSO_4$ (45 g, 374 mmol). Then, *para*-toluene sulfonic acid (*p*TSA, 2.9 g, 15.7 mmol) was added slowly and the mixture was stirred at room temperature for 24 hours. Sodium bicarbonate ($NaHCO_3$, 2.66 g, 31.7 mmol) was added and stirring was continued for 3 h at room temperature. The mixture was filtered, dried over $MgSO_4$ and concentrated under reduced pressure to obtain a white slurry. Water (350 mL) was added and the organic phase was extracted with dichloromethane (DCM) (4 × 200 mL). The organic phase was dried over $MgSO_4$, filtered and concentrated under reduced pressure (25 °C) to obtain the target compound **1** as a slightly yellow liquid (18.6 g, 74%). ^{1}H-NMR (400 MHz, $CDCl_3$): δ 3.95-1.92 p.p.m. (m, 2H), 3.52-3.40 (m, 3H), 2.80 (s, 1H), 1.47-1.24 (m, 12H).

4-(2,2-Dimethyl-1,3-dioxolan-4-yl)butyl methacrylate **2**: 4-(2,2-Dimethyl-1,3-dioxolan-4-yl)butan-1-ol **1** (14.3 g, 82.2 mmol), *N,N*-diisopropylethylamine (DIPEA, 11.7 g, 90.5 mmol), 4-dimethylaminopyridine (DMAP, 100 mg, 0.82 mmol) and methacrylic anhydride (15.2 g, 98.8 mmol) were mixed and stirred for 24 h at room temperature. Methanol (MeOH) (5 mL) was added and the mixture was stirred for additional 3 hours. Heptane (50 mL) and water (50 mL) were added and the organic phase was washed with 0.5 M HCl (3 × 50 mL), 0.5 M NaOH (3 × 50mL) and water (1 × 50mL). Then, the organic phase was dried over $MgSO_4$, filtered and concentrated under reduced pressure at 50 °C to obtain target compound **2** as a slightly yellow liquid (10.0 g, 70%). ^{1}H-NMR (400 MHz, $CDCl_3$): δ 6.03 p.p.m. (s, 1H), 5.49 (s, 1H), 4.09-4.00 (m, 4H), 3.43 (m, 1H), 1.88 (s, 3H), 1.68-1.34 (m, 12H).

5,6-Dihydroxyhexyl methacrylate **3a**: 4-(2,2-Dimethyl-1,3-dioxolan-4-yl)butyl methacrylate **2** (2.0 g, 8.26 mmol) was dissolved in dioxane (50 mL) and THF (5 mL) before HCl (1 M, 0.5 mL and 36% 0.4 mL) was added slowly. The transparent solution was stirred for 48 hours at room temperature and DCM (100 mL) was added. The organic phase was washed with water (3 × 50 mL) and dried over $MgSO_4$, filtered and concentrated under reduced pressure to obtain target compound **3a** as a yellow oil (1.6 g, 80%). ^{1}H-NMR (400 MHz, $CDCl_3$): δ 5.98 p.p.m. (s, 1H), 5.45 (s, 1H), 4.09-3.90 (m, 4H), 3.56-3.27 (m, 3H), 1.81 (s, 3H), 1.68-1.27 (m, 6H).

5,6-Dioxaborolanehexyl methacrylate **3b**: 5,6-Dihydroxyhexyl methacrylate **3a** (2.0 g, 9.89 mmol) was dissolved in THF (20 mL) and mixed with the phenylboronic acid (1.27 g, 10.4 mmol) and $MgSO_4$ (3.8 g, 31.7 mmol). The mixture was stirred for 5 hours at room temperature, filtered and concentrated under reduced pressure to obtain target compound **3b** as a slightly yellow oil (2.2 g, 77%). ^{1}H-NMR (400 MHz, $CDCl_3$): δ 7.80-7.26 p.p.m. (m, 5H), 6.10 (s, 1H), 5.55 (s, 1H), 4.56 (m, 1H), 4.44 (m, 1H), 4.20 (m, 3H), 1.93 (s, 3H), 1.68-1.50 (m, 6H).

Synthesis of bis-dioxaborolane crosslinker

2,2'-(1,4-Phenylene)-bis[4-methyl-1,3,2-dioxaborolane] **4**: Benzene-1,4-diboronic acid (3.0 g, 18.1 mmol) and 1,2-propanediol (2.82 g, 37.1 mmol) were mixed in THF (30 mL) and water (0.1 mL). $MgSO_4$ (5 g) was added. After 24 hours at room temperature, the solution was filtered and concentrated under reduced pressure to obtain the target compound as a slightly yellow solid. Then, the solid was immersed into heptanes and stirred for 1 hour at 50 °C, filtered and concentrated under reduced pressure to obtain target compound **5** as white solid (4.06 g, 91%).

^{1}H-NMR ($CDCl_3$, 400 MHz): δ 7.82 p.p.m. (s, 4H), 4.77-4.69 (m, 2H), 4.46 (dd, J = 8.8 Hz, 1.2 Hz, 2H), 3.90 (dd, J = 8.8 Hz, 1.2 Hz, 2H), 1.41 (d, J = 6.4 Hz, 6H). ^{13}C-NMR (100 MHz, THF-d_8): δ 131.8, 71.9, 70.5, 18.9. Carbon adjacent to boron not detected.

Synthesis of dioxaborolane maleimide

1-[(2-phenyl-1,3,2-dioxaborolan-4-yl)methyl]-1*H*-pyrrole-2,5-dione **6**: Compound **5** was synthesized according to literature (*40*). Compound **5** (5.5 g, 23.1 mmol) and phenylboronic acid (2.8 g, 23.1 mmol) were dissolved in toluene and heated under reflux conditions (T = 135 °C) with Dean-Stark equipment to trap water for 6 hours. Afterwards, the mixture was cooled to room temperature and the solvent was removed under reduced pressure. The residue was dissolved in ethanol and the mixture stored at -5 °C, after which the product crystallized as a yellow solid. Yield = 4.8 g. η = 81%.

^{1}H NMR (DMSO-d_6, 400 MHz): δ 7.66 p.p.m. (d, 2H, J = 8 Hz), 7.51 (t, 1H J = 7.2 Hz), 7.40 (t, 2H, J = 7.6 Hz), 7.07 (s, 2H), 4.75 (ddt, 1H, $^3J_{2,3a}$ = 8 Hz, $^3J_{2,1}$ = 6 Hz, $^3J_{2,3b}$ = 5.6 Hz), 4.39 (dd, 1H, $^2J_{3a,3b}$ = 9.6 Hz, $^3J_{3a,2}$ = 8 Hz), 4.11 (dd, 1H, $^2J_{3b,3a}$ = 9.6 Hz, $^3J_{3b,2}$ 5.6 Hz), 3.67 (d, 2H, $^3J_{1,2}$ = 6 Hz). ^{13}C NMR (DMSO-d_6, 400 MHz): δ 170.9, 134.6, 134.4, 131.5, 127.8, 74.4, 68.5, 41.3. GC ESI-MS: (m/z) calc for $C_{13}H_{12}BNO_4$ 257.09, found 257. FT-IR: 3467, 3098, 3082, 3055, 3027, 2973, 2943, 2908, 1701, 1602, 1500, 1481, 1439, 1398, 1363, 1330, 1315, 1216, 1164, 1095, 1071, 1028, 1001, 980, 894, 828, 801, 765, 695, 658, 644.

Polymerization and characterization of poly(methyl methacrylate) with pending dioxaborolanes

Synthesis of poly(methyl methacrylate) with pending diol functionalities **7**. MMA (15 g, 149.8 mmol), 5,6-dihydroxyhexyl methacrylate **3a** (7.58 g, 37.5 mmol), 2-phenyl 2-propyl benzodithioate (51.0 mg, 0.187 mmol) and AIBN (12.3 mg, 0.075 mmol) were dissolved in anisole (15 mL). The resulting mixture was bubbled with nitrogen at room temperature for 30 minutes before heating up to 65 °C. The reaction mixture was kept under nitrogen while stirring at 65 °C. After 16 hours, THF (10 mL) was added to the viscous oil and the mixture was precipitated from dry diethyl ether (Et_2O). Yield = 17.5 g. Total monomer conversion: 77%. M_n = 71 000 g/mol, M_w = 96 000 g/mol, $Đ$ = 1.35.

Synthesis of poly(methyl methacrylate) with pending dioxaborolanes **8a**. Polymer **7** (17 g, 31.9 mmol diols, 0.274 mmol chains) was dissolved in THF (250 mL) and phenylboronic acid (4.08 g, 33.5 mmol) and water (0.1 mL) were added. After 5 minutes, $MgSO_4$ (11.5 g) was added and the mixture was stirred at room temperature for 5 hours. AIBN (173 mg, 1.06 mmol) was added and the mixture heated for 6 hours at 60 °C

before stirring at room temperature for 9 additional hours. Triphenylphosphine (277 mg, 1.06 mmol) was added and the reaction mixture was stirred at 40 °C for 1 additional hour. The mixture was put in a centrifuge for 30 minutes at 8500 rpm, filtered, concentrated under reduced pressure and precipitated from dry Et_2O. The polymer **8a** was dried at 100°C under high vacuum for 16 hours. Yield = 14.5 g. Ratio Diol/MMA 1/3.3 from conversions: M_n = 86 000 g/mol, M_w = 120 000 g/mol, $Đ$ = 1.40.

Synthesis of poly(methyl methacrylate) with pending dioxaborolanes **8b**. MMA (1.22 g, 12.2 mmol), 5,6-dioxaborolane methacrylate **3b** (880 mg, 3.05 mmol), 2-phenyl 2-propyl benzodithioate (16.7 mg, 0.061 mmol) and AIBN (4.0 mg, 0.024 mmol) were dissolved in anisole (1.2 mL). The resulting mixture was bubbled with nitrogen at room temperature for 30 minutes before heating up to 65 °C. The reaction mixture was kept under nitrogen while stirring at 65 °C. After 16 hours, THF (1 mL) was added to the viscous oil and the mixture was precipitated from dry Et_2O. Yield = 1.2 g. M_n = 24 300 g/mol, M_w = 28 600 g/mol, $Đ$ = 1.18.

Synthesis of poly(methyl methacrylate) with pending diol functionalities **9**. MMA (26 g, 259.7 mmol), 5,6-dihydroxyhexyl methacrylate **3a** (13 g, 65 mmol), Styrene (1.3 g, 12.9 mmol), 2-phenyl 2-propyl benzodithioate (88.2 mg, 0.324 mmol) and AIBN (21.3 mg, 0.130 mmol) were dissolved in anisole (15 mL). The resulting mixture was bubbled with nitrogen at room temperature for 30 minutes before heating up to 65 °C. The reaction mixture was kept under nitrogen while stirring at 65 °C. After 20 hours, THF (10 mL) was added to the viscous oil and the mixture was precipitated from dry Et_2O. Yield = 28 g. Total monomer conversion: 72%. Ratio S/Diol/MMA from NMR: 1/4/15; M_n = 78 000 g/mol, M_w = 95 000 g/mol, $Đ$ = 1.21.

Synthesis of poly(methyl methacrylate) with pending diol functionalities **10** (removal of chain ends). Polymer **9** (28 g, 0.324 mmol chains) was dissolved in a 1/1 THF/dimethylformamide (DMF) mixture (400 mL) and reacted with *n*-butyl amine (118 mg, 1.62 mmol) at room temperature under argon for 5 hours. *n*-Butylacrylate (2.07 g, 16.2 mmol) was added to the reaction mixture and stirring was continued for 18 hours at room temperature. The mixture was concentrated under reduced pressure and the colorless polymer **10** was precipitated from diethylether (26 g). M_n = 80 000 g/mol, M_w = 94 000 g/mol, $Đ$ = 1.2.

Synthesis of poly(methyl methacrylate) with pending dioxaborolanes **11**. Polymer **10** (15 g, 24.7 mmol diols) was dissolved in THF (250 mL) and reacted with phenylboronic acid (3.4 g, 32.0 mmol) and water (0.1 mL) were added. After 5 minutes, $MgSO_4$ (11.5 g) was added and the mixture was stirred at room temperature for 5 hours. The mixture was put in a centrifuge for 30 minutes at 8500 rpm, filtered, concentrated under reduced pressure and precipitated from dry Et_2O. The polymer **11** was dried at 100 °C under high vacuum for 16 hours. Yield = 14 g. M_n = 85 000 g/mol, M_w = 102 000 g/mol, $Đ$ = 1.2.

Synthesis of poly(methyl methacrylate)

MMA (15 g, 149.8 mmol), styrene (0.78 g, 7.5 mmol), 2-phenyl 2-propyl benzodithioate (51 mg, 0.187 mmol) and AIBN (12.3 mg, 0.075 mmol) were dissolved in anisole (15 mL). The resulting mixture was bubbled with nitrogen at room temperature for 30 minutes before heating up to 65 °C. The reaction mixture was kept under nitrogen while

stirring at 65 °C. After 16 hours, THF (15 mL) was added to the viscous oil and the mixture was precipitated from dry diethyl ether. Yield = 11 g. Total monomer conversion: 70%. M_n = 84 000 g/mol, M_w = 101 000 g/mol, $Đ$ = 1.2.

Polymerization and characterization of polystyrene with pending dioxaborolanes

Synthesis of polystyrene with pending diol functionalities **12**. Styrene (43 mL, 376 mmol), 5,6-dihydroxyhexyl methacrylate **3a** (7.6 g, 37.6 mmol) and 2-phenyl 2-propyl benzodithioate (102 mg, 0.376 mmol) were mixed with anisole (0.7 mL, internal standard) and bubbled with argon at room temperature for 30 minutes. The mixture was heated to 140 °C for 6 hours and samples were taken to follow the reaction kinetics. After 6 hours, the mixture was diluted with THF and precipitated from MeOH. The polymer was filtered and dried under reduced pressure to obtain a pink solid **12** (35 g, yield weight 75%). Conversion of diol methacrylate = 85.7%, conversion of styrene = 73.1%, ratio diol methacrylate/styrene from conversions: 1/8.5. M_n = 75 000 g/mol, M_w = 118 000 g/mol, $Đ$ = 1.57.

Synthesis of polystyrene with pending diol functionalities **13** (removal of chain ends). Polymer **12** was dissolved in a 1/1 THF/DMF mixture (250 mL) and reacted with *n*-butyl amine (275 mg, 3.76 mmol) at room temperature under argon for 5 hours. *n*-Butylacrylate (4.8 g, 37.6 mmol) was added to the reaction mixture and stirring was continued for 18 hours at room temperature. The mixture was concentrated under reduced pressure and the colorless polymer **12** was precipitated from MeOH (ca. 30 g). M_n = 77 000 g/mol, M_w = 123 000 g/mol, $Đ$ = 1.60.

Synthesis of polystyrene with pending dioxaborolanes **14**. The polymer **13** (25 g, 23.8 mmol pending diols) was dissolved in THF (50 mL) and phenylboronic acid (2.94 g, 24.1 mmol) and $MgSO_4$ (8.68 g, 72.4 mmol) were added. After 5 hours at room temperature, the mixture was put in the centrifuge and then filtered, concentrated under reduced pressure and precipitated from dry Et_2O to yield polymer **14**. M_n = 76 000 g/mol, M_w = 130 000 g/mol, $Đ$ = 1.71.

Crosslinking in solution

Poly(methyl methacrylate) with pending dioxaborolanes **8** and **11** (10 g) or polystyrene with pending dioxaborolane **14** (10 g) was dissolved in dry THF (25 mL) and a solution of the bis-dioxaborolane crosslinker **4** (220 mg) in dry THF (0.5 mL) was added. Gel formation was observed after 10-30 minutes at room temperature. The gel was dried under vacuum at 120 °C for 5 hours, ground and further dried for 16 additional hours at 120 °C under vacuum. This process distillates out all remaining free dioxaborolane $\mathbf{B_1}$-$\mathbf{D_2}$ formed during the crosslinking reaction.

b. Solubility characterization of dioxaborolane vitrimers from vinylic monomers

Swelling tests and cleavage by diolysis of boronic ester vitrimers made from vinyl monomers

Samples were immersed in dried solvent at room temperature and weighted after a characteristic time. Then, they were dried under vacuum at 120 °C until complete dryness. Samples of the respective vitrimer (50-250 mg polymer, n eq. boronic esters) were put in THF and 1,2-propanediol (50-150 n eq.) was added. After one night at room temperature, all tested samples were dissolved completely.

Equation S3
Swelling ratio and soluble fraction of vitrimers

$$Swelling\ ratio = \frac{Mass\ swollen - Mass\ dried}{Mass\ dried}$$

$$Soluble\ fraction = 1 - (\frac{Mass\ dried}{Mass\ dry})$$

5. Rheology studies of dioxaborolane vitrimers from vinylic monomers

Viscoelastic properties of poly(methyl methacrylate) and polystyrene samples were determined using a TA Instruments ARES G2 rotational rheometer equipped with parallel plate geometry (25 mm in diameter) in a convection oven under air.

a. Step stress-creep recovery

Creep-recovery tests were carried out between 130 °C and 200 °C by imposing a constant stress over time (creep) and releasing it for a certain period of time (recovery) while measuring the strain. The linear part of variation of the strain versus time of the creep-recovery plots were fitted using linear regression. The shear creep compliance J_{eq} was determined from the intercept of the linear fit. The strain rate $\dot{\gamma}$ was determined from the slope of the linear fit. The viscosity η and the relaxation time τ were calculated from:

Equation S4

$$\eta = \frac{\sigma}{\dot{\gamma}}$$

Equation S5

$$\tau = \eta J_{\mathrm{eq}}$$

b. Stress relaxation:

Stress relaxation measurements on poly(methyl methacrylate) samples were conducted between 120 °C and 160 °C by applying a constant shear strain of 1%. The zero-shear viscosity η_0 and the relaxation time τ were calculated from stress relaxation experiments as:

Equation S6

$$\eta_0 = \int_0^\infty G(t)dt$$

Equation S7

$$\tau = \frac{\int_0^\infty t\, G(t)dt}{\int_0^\infty G(t)dt}$$

c. Frequency sweep:

Frequency sweeps were performed from 100 to 0.01 rad/s at 200 °C with a constant strain amplitude of 1%. Complex viscosities ($|\eta*|$) were determined at 2 10^{-2} rad/s. Relaxation times were determined from the frequency of crossover of G' and G''.

6. Thermo-mechanical studies of dioxaborolane vitrimers

a. Calorimetry

Glass, melting and crystallization transitions of materials were determined by differential scanning calorimetry (DSC). Sequences of temperature ramps (heating, cooling, heating) in the 30 °C – 220 °C range for HDPE and in the -25 °C – 220 °C range for poly(methyl methacrylate) and polystyrene were performed at 10 °C/min using a TA Instruments Q1000. The first heating ramp was performed to reset the sample's thermo-mechanical history. The degree of crystallinity χ_c was calculated from the specific enthalpy of melting ΔH_m as $\chi_c = \Delta H_m / \Delta H_m^+$, where $\Delta H_m^+ = 288$ J g^{-1} corresponds to the specific enthalpy of melting of a fully crystalline polyethylene (*43*).

b. Tensile tests

Uniaxial tensile tests were performed on dumbell-shaped specimens using an Instron 5564 tensile machine mounted with a 2 kN cell and equipped with an oven. Specimens were tested in quintuplicates at a fixed crosshead speed of 10 mm/min (HDPE) and at 1.5 mm/min (PMMA and PS). Testing was carried out at room temperature for all materials, and HDPE materials were also tested at 80 °C. In the latter case, samples were left to equilibrate at 80 °C for 3 min prior to testing. Engineering stress-strain curves were obtained according to ISO 527-1 standard through measurements of the tensile force F and crosshead displacement Δl by defining the engineering stress as $\sigma = F/S_0$ and the strain as $\gamma = \Delta l / l_0$, where S_0 and l_0 are the initial cross-section and gauge length of the specimens, respectively. The Young's modulus was determined as the initial slope of the engineering stress-strain curves. For HDPE materials the ultimate tensile strength was determined as the local maximum in engineering stress at the elastic–plastic transition. For PMMA and PS materials the engineering stress at break was considered. Following tensile testing, the vitrimer specimens were cut down to small fragments and reshaped via compression molding (HDPE) or injection molding (PMMA and PS) in order to test their recyclability over several reprocessing cycles. Tensile tests were repeated at room temperature for each generation.

Tensile creep resistance tests were performed at 80 °C on HDPE and HDPE vitrimers using the aforementioned setup. After 3 min of equilibration at 80 °C, samples were subjected to a constant crosshead speed of 10 mm/min until the engineering stress reached 5 MPa, which was subsequently maintained for at least 60 000 s (Fig. S43). The 5 MPa stress was reached in approximately 7 s after the onset of the test. The creep values reported in Fig. 4B correspond to the increase in creep deformation between 10 000 s and 60 000 s. These values were averaged over at least 4 tests on different specimens for reproducibility.

c. Dynamic mechanical analysis

Dynamic mechanical analysis was carried out using a TA Instruments Q800 in tension mode. Temperature ramps were performed at a constant rate of 3 °C/min from -50 °C to 260 °C for HDPE materials and from -25 °C to 220 °C for poly(methyl

methacrylate) and polystyrene samples with a maximum strain amplitude of 1% at a fixed frequency of 1 Hz.

7. Polyethylene dioxaborolane vitrimer synthesis and chemical characterization

Reactive melt grafting and bulk crosslinking

Functionalization of HDPE was carried out using a DSM Explore batch twin-screw extruder (5 cm^3 capacity) equipped with co-rotating conical screw profile and recirculation channel to control the residence time. The force applied by the sheared material on the barrel of the extruder was recorded over time (once the sheared material is in the molten state, that force gives an indirect measure of the melt viscosity). Melt grafting and bulk crosslinking were performed in two steps under nitrogen atmosphere with a barrel temperature of 170 °C and a screw speed of 100 rpm. First, a dry blend of HDPE, dioxaborolane maleimide (4 wt%) and dicumyl peroxide (0.05 wt%) was mixed in plastic bottles prior to introduction in the extruder. An increase in viscosity was observed over approximately 3 min prior to reaching a plateau region. For thermoplastic dioxaborolane functionalized HDPE **15,** the polymer was driven out of the extruder through a circular die after a total residence time of 8 minutes (Fig S29). For HDPE vitrimers, the crosslinker compound **4** was introduced in the extruder after 8 min in residence time. The effect of the crosslinker was marked by an increase in viscosity over approximately 1 min, followed by a decrease over approximately 3 min prior to level off. The material was driven out of the extruder through a circular die after a total residence time of 14 min. The extrudate looked smooth and transparent at the die exit prior to crystallization at room temperature (Fig S36).

The same procedure was also attempted using the diol maleimide **5b** instead of dioxaborolane maleimide **6** to yield linear diol functionalized HDPE **17** (Fig S34). Although the grafting of the molecule along the HDPE backbone was successful, no effect of the crosslinker addition on the viscosity could be observed and the molten material came out of the die as an opaque extrudate with a pronounced orange coloration (Fig S36).

Crosslinking of polystyrene with pending dioxaborolanes **14** was performed in the presence of the diboronic ester crosslinker **4** in 2.2 wt% with a barrel temperature of 200 °C, a screw speed of 100 rpm and residence time of 6 min. Extrudates were collected and let to cool down to room temperature.

For both HDPE and PS vitrimers prepared by bulk crosslinking during extrusion, no further high vacuum treatment at elevated temperatures was utilized. Dioxaborolane $\mathbf{D_1}$-$\mathbf{B_1}$ that is formed in the crosslinking process remains inside the polymer network.

Synthesis of poly-maleimide **16**

1-[(2-phenyl-1,3,2-dioxaborolan-4-yl)methyl]-1*H*-pyrrole-2,5-dione **6** (200 mg, 0.78 mmol) and dicumyl peroxide (10 mg, 0.037 mmol) were dissolved in trichlorobenzene (1 mL) and heated at 170 °C for 10 minutes. The resulting highly viscous solution was precipitated from hexane to give a yellow powder, which was filtered and subsequently dried in vacuo to yield polymaleimide **16**. Yield = 184 mg, η = 92 %. ^{1}H NMR ($CDCl_3$, 400 MHz): δ 7.8-7.2 p.p.m. (b, 5H, aromatic), 4.9-3 (b, 7H, aliphatic). M_n = 20600 g/mol, M_w = 57400 g/mol, $Đ$ = 2.8.

FT-IR spectroscopic analysis of maleimide grafting onto HDPE

To confirm the radical induced grafting of maleimide **6** onto HDPE, FT-IR spectroscopic analysis was used. Specifically, the C-H out of plane bending vibration of the maleimide double bond at 830 cm^{-1} was monitored. The FT-IR spectra of HDPE, maleimide **6**, a physical mixture of HDPE and maleimide **6** and grafted HDPE **15** were recorded (Fig. S32). The disappearance of the maleimide C-H out of plane bending vibration upon radical induced grafting during extrusion suggests the complete consumption of all the maleimide present in the polymer mixture. To assess the side reaction of polymerization of maleimide **6** into polymaleimide **16** that potentially competes with grafting onto PE during reactive extrusion; we synthesized polymaleimide **16** in solution. The isolated polymer readily dissolves in organic solvents such as acetone, chloroform and THF. To purify grafted HDPE **15** from unreacted maleimides and side-products, a piece of polymer was dissolved in *ortho*-dichlorobenzene (ODCB) at 140 °C. The resulting solution was precipitated into acetone and subsequently washed three times with boiling acetone, after which the polymer was dried under vacuum. As maleimide **6** and polymaleimide **16** are both soluble in acetone, the purification procedure of grafted HDPE **15** should result in the complete removal of both species. FT-IR spectra were recorded for the purified **15** and compared to the as-extruded polymer (Fig. S33). The efficiency of the grafting reaction was estimated by the carbonyl vibration of the maleimide fragment (1700 cm^{-1}) to the C-H bending vibration of the HDPE polymer (1470 cm^{-1}) in the as-extruded sample and the purified polymer. The results suggest a complete grafting of the maleimide onto the HDPE polymer. A similar procedure was followed for the characterization of HDPE with pending diols **17** that was prepared by grafting with diol maleimide **5b** (Figs. S34 and S35). The spectral comparison between as-extruded HDPE **17** and maleimide **5b** indicates the complete disappearance of the C-H out of plane bending vibration of the maleimide fragment, suggesting successful grafting of **5b** onto the HDPE backbone.

8. Properties of polyethylene dioxaborolane vitrimer

a. Solubility tests

Determination of gel content

The gel content of HDPE vitrimers was determined according to ISO 10147 standard procedure. Typically, a vitrimer sample of approximately 0.24 g was placed in stainless steel fine wire cage of known weight and subsequently immersed in dried xylene as the solvent (the solvent weight was 200 times that of the sample). Soxhlet extraction was carried out at 140 °C for 8 hours in the presence of an antioxidant (Irganox 1010, 10 wt% respective to the solvent weight), after which the cage was washed in boiling dried xylene in order to remove any dissolved residue. Next the cage was dried at 140 °C under vacuum for 3 hours. The remaining dried gel was weighted and the gel content was calculated as the dried gel mass to initial sample mass ratio.

In order to discriminate the presence of a permanent non-dynamic covalent network within the samples, reactive cleavage of the network was performed using a similar procedure, but this time adding 1,2-octanediol to the solvent and antioxidant. HDPE vitrimers showed an average gel content of 31.7%, while Soxhlet extraction in the presence of excess 1,2-octanediol resulted in the full dissolution of the samples (Table S8). The presence of 1,2-octanediol results in the diolysis of the dioxaborolane cross-links and in the formation of soluble linear polymers (Fig. S44). As control experiments, Soxhlet extractions were performed on HDPE, HDPE treated with 0.05 wt% dicumyl peroxide and HDPE with pending dioxaborolanes **15**. The Soxhlet extractions confirmed the full solubility of these linear polymers in boiling xylene. The synthesis of PE vitrimers by diol/dioxaborolane exchange was also attempted by grafting of diol maleimide **5b** onto HDPE and subsequent cross-linking with bis-dioxaborolane **4**. Soxhlet extractions on HDPE with pending diols **16** and on the potential corresponding vitrimer showed the full solubility of the linear grafted polymer and the supposed network, indicating that no chemical network was formed by diol/dioxaborolane exchange during the reactive extrusion process.

b. Melt flow index

Melt flow index measurements

Fluidity tests of HDPE materials were carried out using a Kayeness 7054 melt flow indexer. The melt flow index (MFI) was determined according to ISO 1133 standard. A melt temperature of 190 °C was used for all samples. The applied weight was 2.16 kg for the starting HDPE and 10 kg for the grafted HDPEs and HDPE vitrimers (Table S8). The MFI values were averaged over at least 4 measurements.

c. Stress relaxation

Rheological characterization of polyethylene materials

Viscoelastic properties of HDPE-based materials were determined using an Anton Paar MCR501 rotational rheometer equipped with parallel plate geometry (25 mm in diameter) in a convection oven under nitrogen flow. Stress relaxation measurements on

HDPE-based materials were conducted at 190 °C by applying a constant shear strain of 1%.

9. Environmental stress cracking

Environmental stress cracking of PS materials was performed using a TA Instruments Q800 in three point bending geometry. Rectangular samples prepared by compression molding at 150 °C for 5 minutes were used. Their dimensions were : length of 30 mm, width of 15.8 mm, thickness of 1.4 mm. Environmental conditions were simulated by placing the samples on the two lower tips of a demounted three point bending set-up in a closed beaker containing a mixture of 300 mL of ethanol/water (9/1). Stress was applied by positioning weights in the center of the samples for different time intervals. The samples were removed, dried on both sides with a paper towel and left at room temperature for 20 more minutes before testing their mechanical resistance. They were subsequently placed in a three point bending set-up and the force was ramped at 3 N/min to 18 N (maximum limit of the machine) at 35 °C.

10. Water uptake of PMMA, PMMA-diol networks, and PMMA dioxaborolane vitrimers

The hydrolytic stability of PMMA vitrimers in contact with water was assessed by performing water uptake tests. Square pieces of polymer of approximately 100 mg weight were cut from compression molded plates of the polymers. The samples were placed in closed vials with distilled water (5 mL) and allowed to take up water at room temperature (16 °C). After seven days, the samples were removed from the water and contact-dried with absorbing paper, after which their weights were recorded. The samples were allowed to further dry to air atmosphere at room temperature (16 °C) for three days, after which their weights were recorded again. Subsequently, the samples were subjected to swelling in anhydrous THF (5 mL) for two days. The solvent was removed and the remaining gels were subjected to drying under vacuum at 120 °C for 15 hours, after which the weights of the insoluble fractions were recorded. The experiment was performed on PMMA V5, PMMA-diol V5 and PMMA (Tables S10-12)

A clear difference is observed in the water uptake of PMMA vitrimers/networks bearing pending diols or dioxaborolanes. At room temperature, the water uptake of PMMA V5 is comparable (2.0±0.9 wt%) to the water uptake observed for conventional PMMA (1.8±0.9 wt%), while PMMA-diol V5 shows a significantly higher water uptake (9.5±1.2 wt%). The difference in water uptake reflects the more hydrophilic nature of the PMMA-diol network as compared to PMMA vitrimer V5. The difference in water uptake between PMMA V5 and PMMA-diol V5 is also reflected in the subsequent swelling experiments in THF. After swelling in THF at room temperature for two days, PMMA V5 samples show an average gel content of 89.9±5.5 %, while PMMA-diol V5 shows a much lower average gel content of 19.0±4.9%. These results indicate a significant effect of the higher water uptake of PMMA-diol V5 on the stability of the dioxaborolane network. The higher propensity for water uptake of PMMA-diol V5 can result in hydrolysis of dioxaborolanes during both the water uptake experiments and the swelling experiments in THF.

11. Adhesion of PMMA and HDPE dioxaborolane thermoplastics and vitrimers

Films of PMMA V5 and HDPE vitrimers were compression molded and cut into strips of 25 mm in length (*L*), 16 mm in width (*w*) and 1.5 mm in thickness (*h*). Lap joints consisting of two single laps were prepared by placing one strip of PMMA-V5 vitrimer onto two separated strips of HDPE vitrimers, with both overlap lengths l_0 equal to 1 cm. The HDPE vitrimer strips were placed in a polytetrafluoroethylene (PTFE) frame with a PTFE spacer between them (Fig. S46 bottom). The lap joints were heated at 190 °C in an oven with a weight of 448 g placed on top of the PMMA vitrimer layer in order to ensure contact in both overlap areas over a given duration (referred to as the *contact time*). The weight was then removed and the lap joints were left to slowly cool down to room temperature prior to testing. Control experiments were performed with the thermoplastic precursors that bear pending dioxaborolanes (polymers **15** and **8a**). An additional PTFE frame was used for the PMMA thermoplastic layer in order to prevent the deformation of the polymer strip during heating (Fig. S46 top). Two contact times were tested (10 min and 20 min). Lap-shear tests were performed with a speed of 10 mm/min using an Instron 5564 tensile machine mounted with a 2 kN cell. The distance between grips was 27 mm.

The adhesion energy G_{adh} was calculated from the interfacial failure force F, using $G_{adh} = (F/w)^2\left(E_2h_2/\left(2E_1h_1(E_1h_1 + E_2h_2)\right)\right)$ for $E_1h_1 < E_2h_2$, where E_1 and E_2 are the Young's moduli, h_1 and h_2 are the thicknesses and w is the width of the stripes, with "1" corresponding to the HDPE vitrimer and "2" corresponding to the PMMA vitrimer (*42, 43*).

Equations S1-S7

Equation S1
Determination of the maximum diol content in boronic esters **B_1-D_2** and **B_2-D_1**

$$[diol]_{max}(\%) = \frac{[diol]_{max}}{\langle [diol]_{max} + [boronic\ ester] \rangle}$$

$$= \frac{0.1\ \text{mM}}{\langle 0.1\ \text{mM} + 1000\ \text{mM} \rangle} = 0.01$$

Equation S2

$$\frac{d[B_1D_1]}{dt} = -\frac{d[B_1D_2]}{dt} = k[B_1D_2][B_2D_1] - k[B_1D_1][B_2D_2]$$

With $[B_1D_2] = [B_2D_1]$ and $[B_1D_1] = [B_2D_2]$

Equation S3
Swelling ratio and soluble fraction of vitrimers

$$Swelling\ ratio = \frac{Mass\ swollen - Mass\ dried}{Mass\ dried}$$

$$Soluble\ fraction = 1 - (\frac{Mass\ dried}{Mass\ dry})$$

Equation S4

$$\eta = \frac{\sigma}{\dot{\gamma}}$$

Equation S5

$$\tau = \eta J_{\text{eq}}$$

Equation S6

$$\eta_0 = \int_0^\infty G(t)dt$$

Equation S7

$$\tau = \frac{\int_0^\infty t\ G(t)dt}{\int_0^\infty G(t)dt}$$

Figures S1-S49

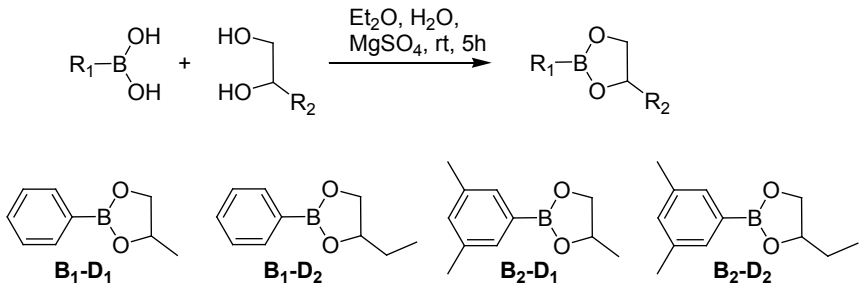

Fig. S1
General synthetic procedure for the preparation of dioxaborolanes.

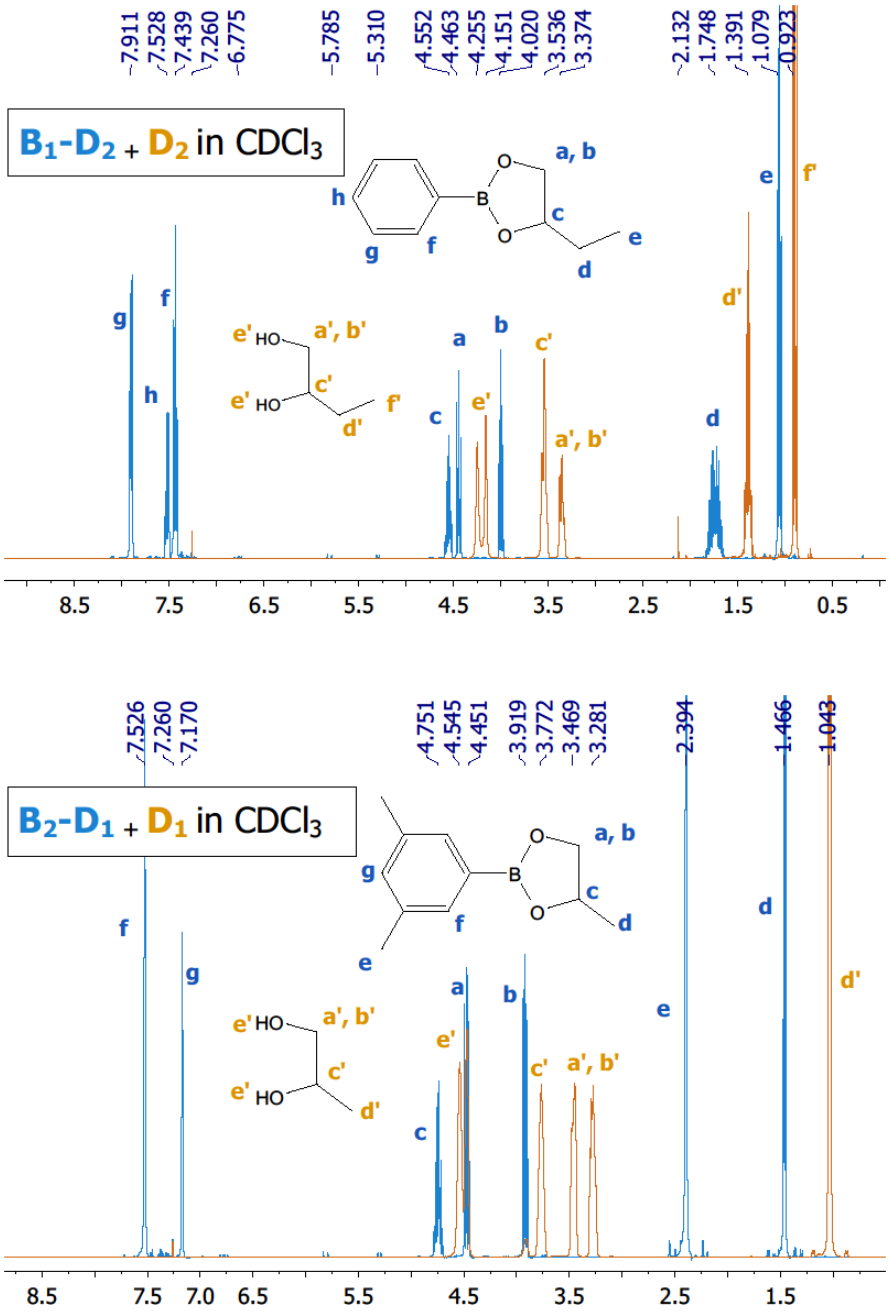

Fig. S2
^{1}H-NMR spectra of highly concentrated solutions of **B_1-D_2** (1 M, top) and **B_2-D_1** (1 M, bottom) in $CDCl_3$ and the overlay with the ^{1}H-NMR spectra of their respective free diols **D_2** and **D_1**. Styrene was added as internal standard (25 mM).

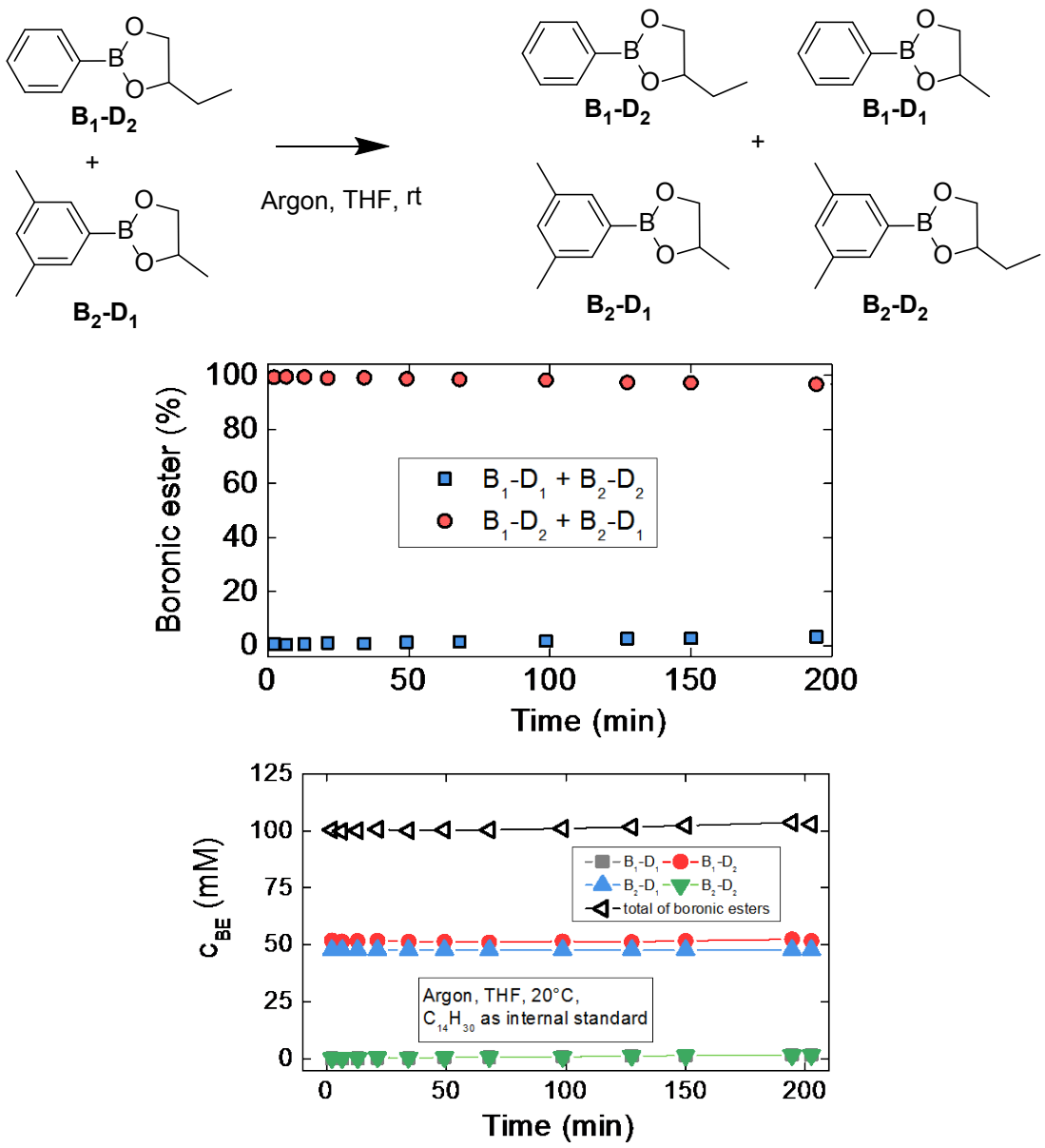

Fig. S3

Kinetic data for the mixing of dioxaborolanes **B_1-D_2** and **B_2-D_1** in THF at 20 °C under argon protective atmosphere. Signals are referred to the internal standard tetradecane and are given in mol% (top, plotted are the sums of reactants and products) and in concentration (bottom, individual curves for each species). No exchange reaction or hydrolysis was detected after 200 minutes under these conditions.

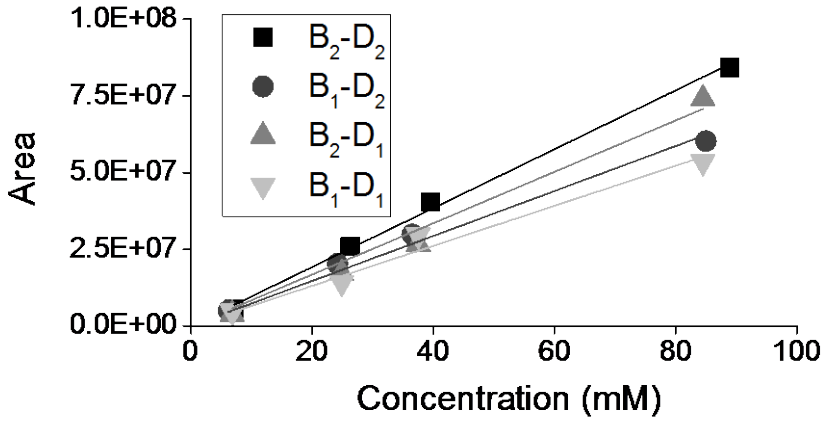

Fig. S4
Calibration curves of dioxaborolanes for gas chromatography characterization and kinetics measurements.

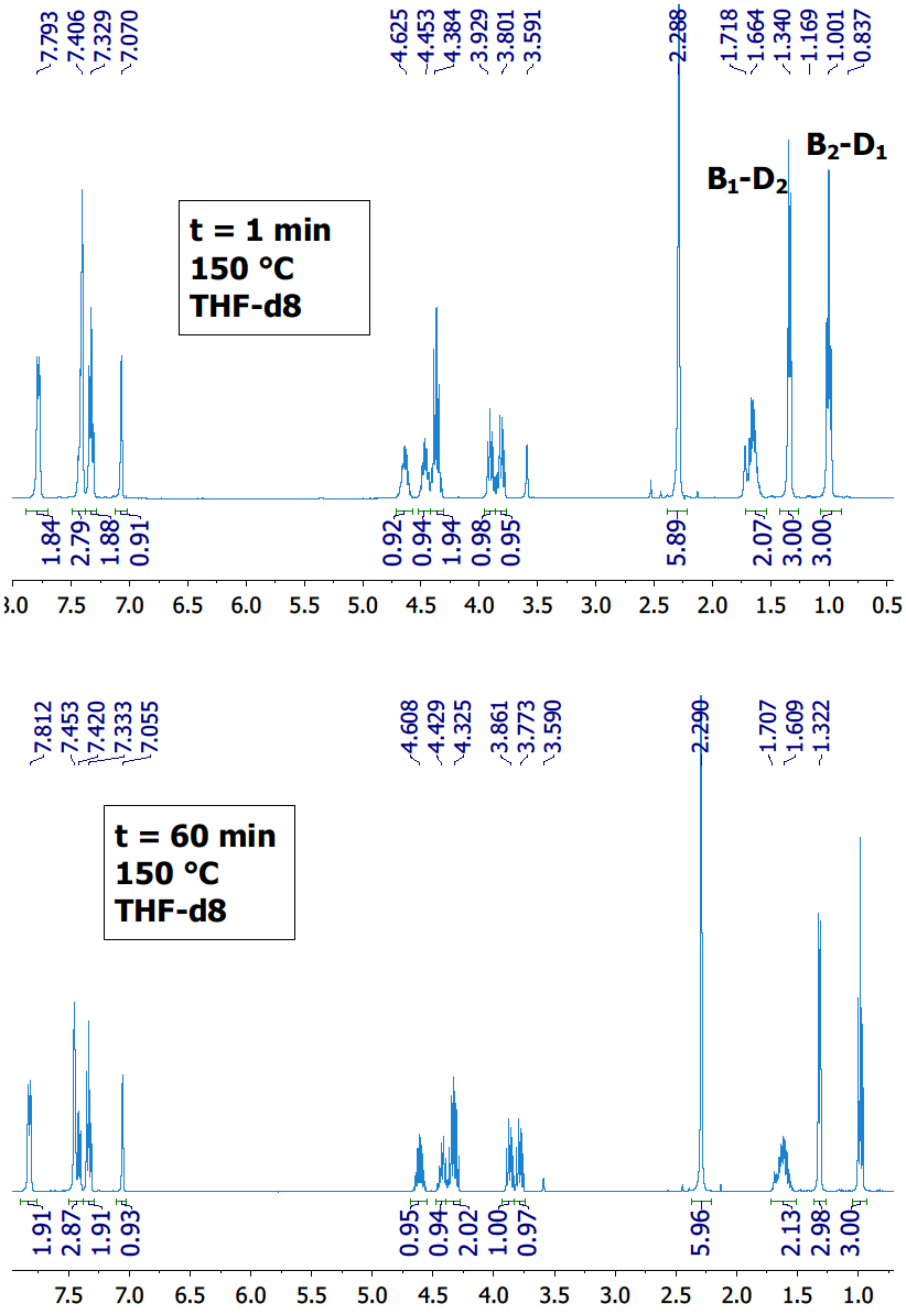

Fig. S5
^{1}H-NMR spectra at 1 minute (top, first data point) and 60 minutes (bottom, at equilibrium) after mixing dioxaborolanes **B_1-D_2** and **B_2-D_1** at 150 °C under argon protective atmosphere.

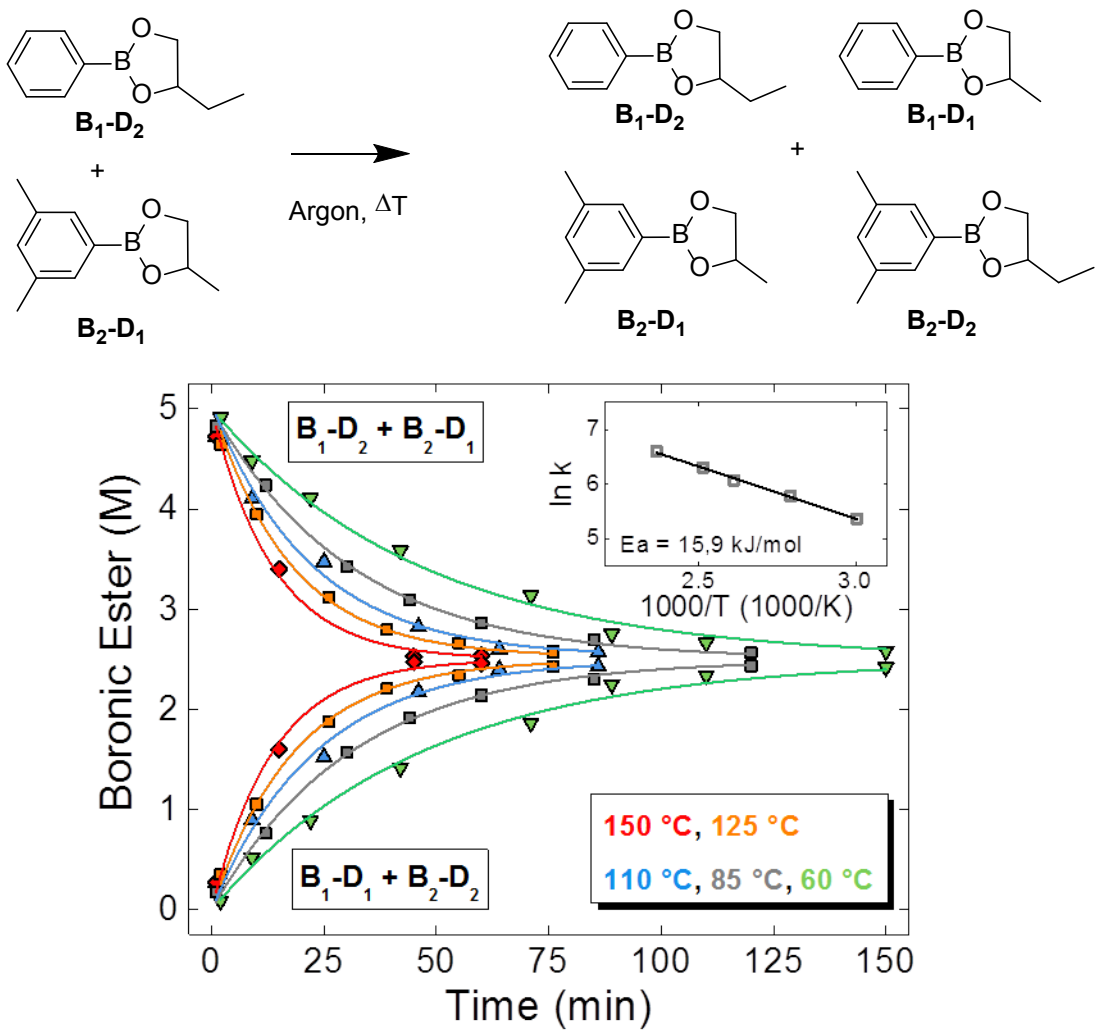

Fig. S6
Kinetic data of the metathesis of dioxaborolanes **B_1-D_2** and **B_2-D_1** in bulk under argon protective atmosphere. For clarity, the reaction kinetics are plotted as the sum of reactants and products. The kinetics of the exchange reaction are fitted with a second order model and assuming a single metathesis rate k ($L.mol^{-1}.s^{-1}$). The activation energy determined from the logarithmic plot of the respective rate constants versus the inverse temperature was estimated to be 15.9 ± 0.45 kJ/mol. A second order model was used to fit the kinetics of dioxaborolane metathesis. A single metathesis rate is assumed.

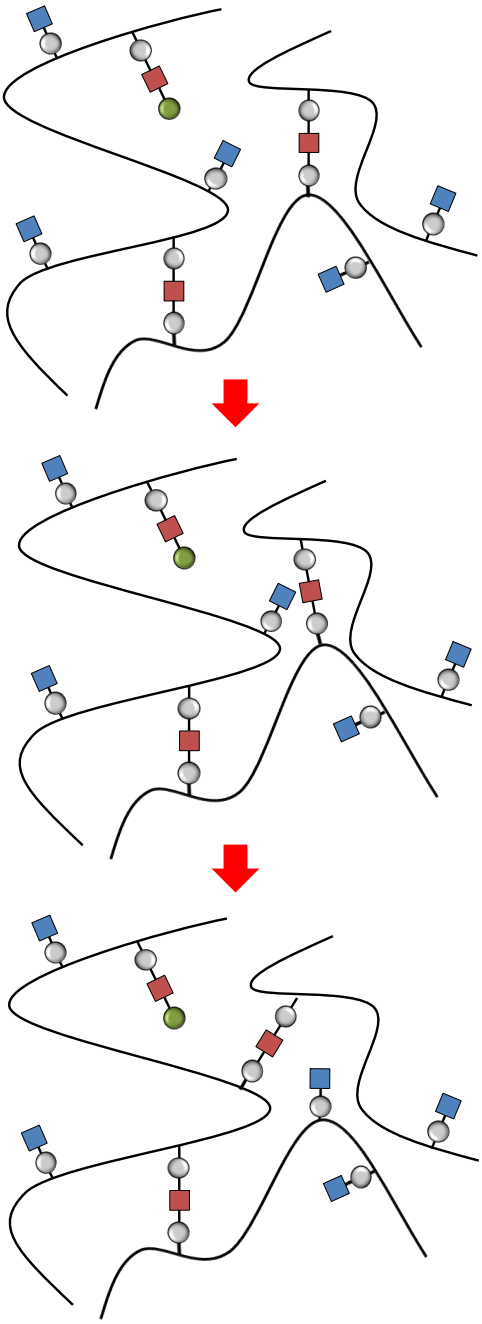

Fig. S7
Topological rearrangements via metathesis of dioxaborolanes preserving the integrity and connectivity of the vitrimer network. The situation depicted here corresponds to the situation in which free dioxaborolanes generated during crosslinking were removed by evaporation after synthesis.

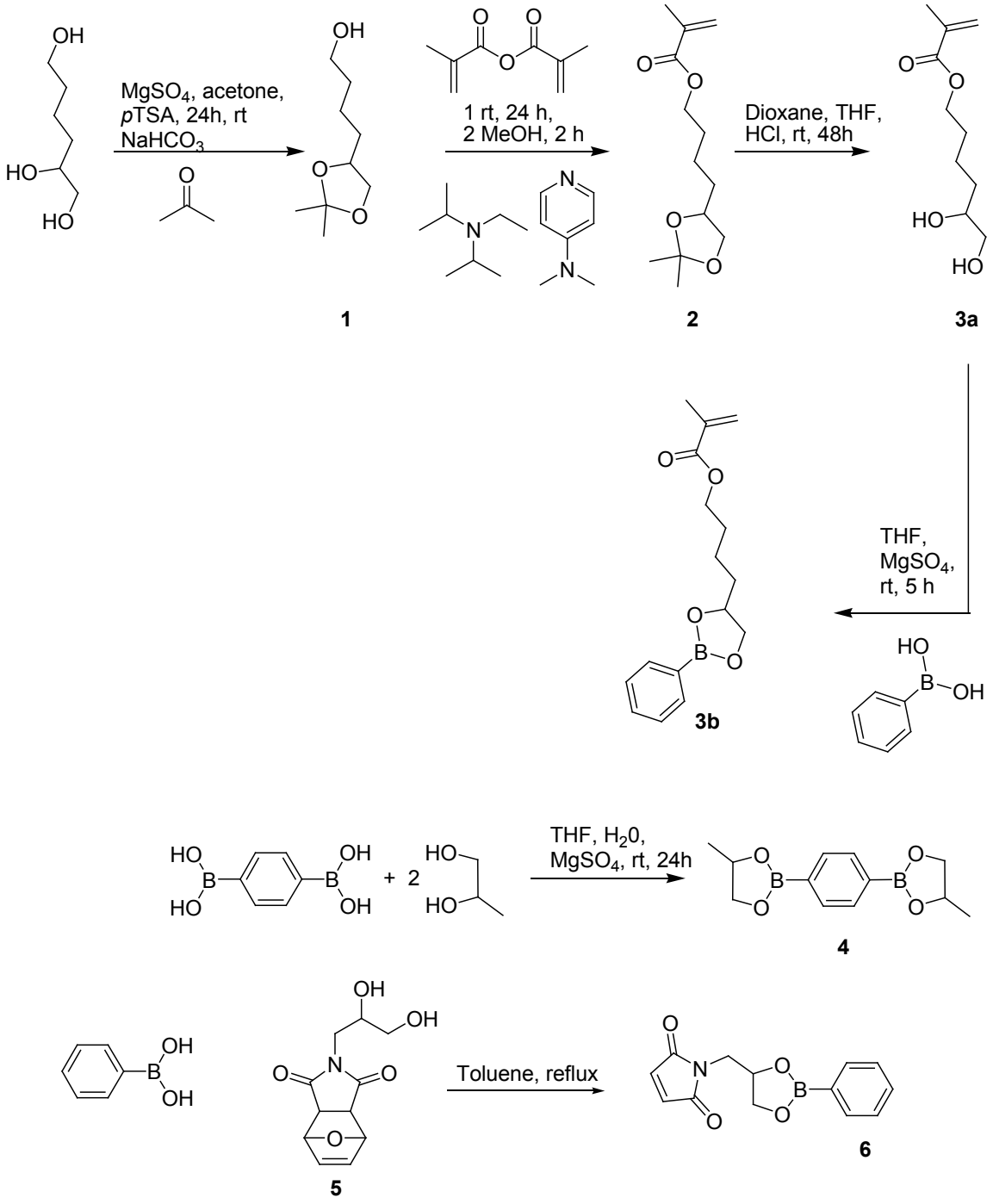

Fig. S8

Synthetic procedures for the generation of functional monomers 5,6-dihydroxyhexyl methacrylate (**3a**), 5,6-dioxaborolane methacrylate (**3b**), bis-dioxaborolane 2,2'-(1,4-phenylene)bis[4-methyl-1,3,2-dioxaborolane] crosslinker (**4**) and dioxaborolane functionalized maleimide (**6**).

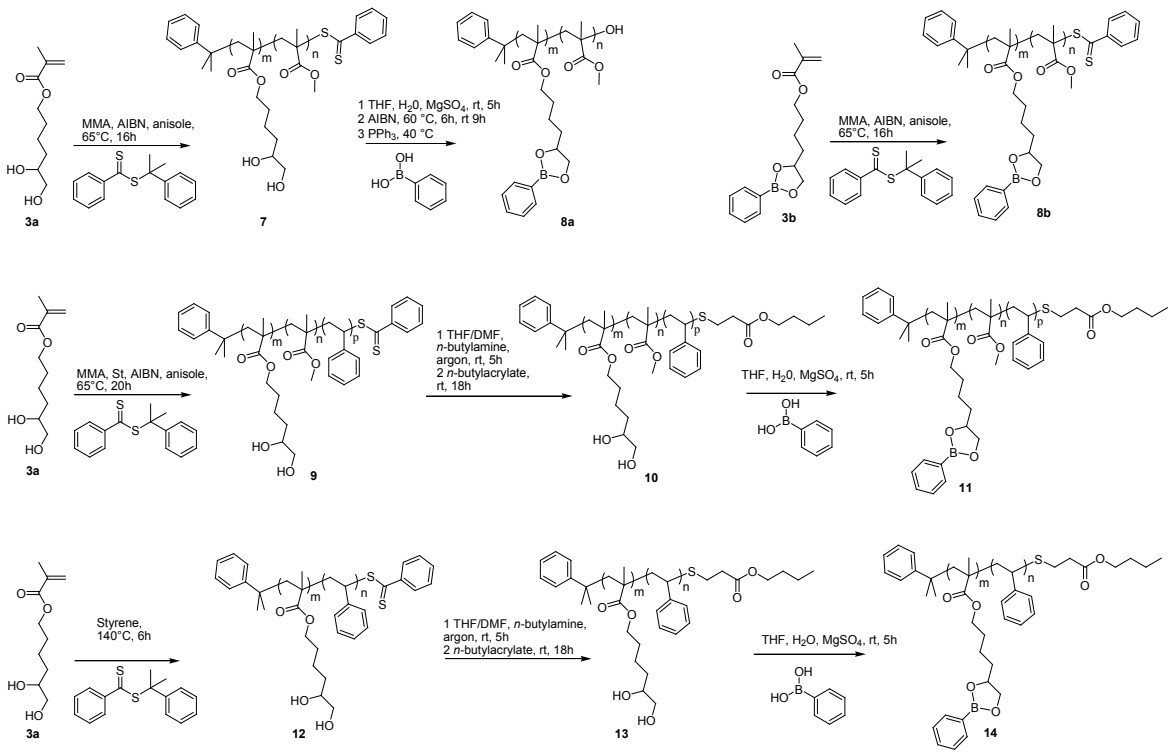

Fig. S9

Synthesis of poly(methyl methacrylate) with pending dioxaborolanes (**8a**, **8b** and **11**), and polystyrene with pending dioxaborolanes (**14**).

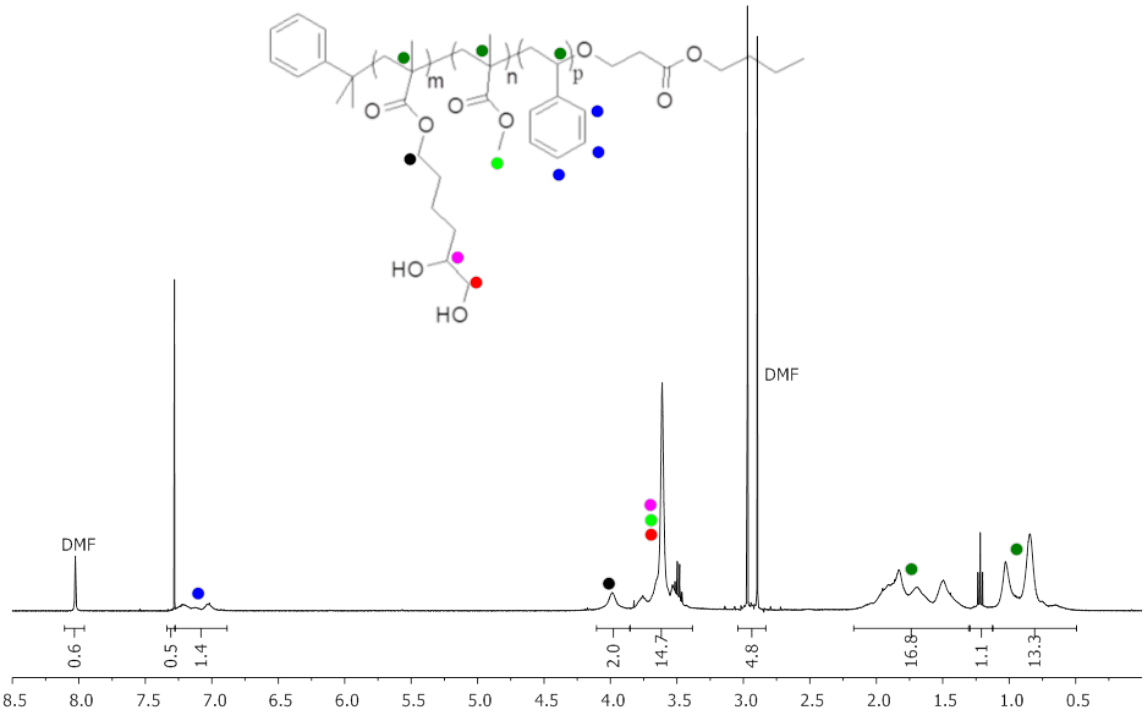

Fig S10
^{1}H-NMR spectrum of PMMA with pending diol functionalities **10** in $CDCl_3$.

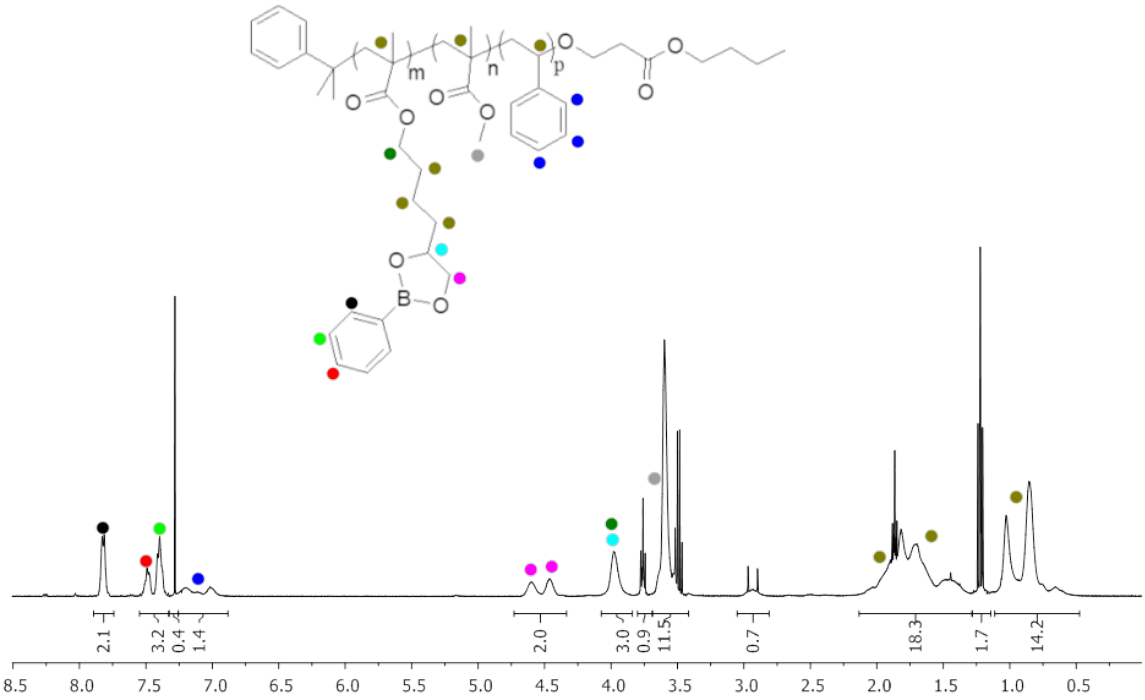

Fig S11
^{1}H-NMR spectrum of PMMA with pending dioxaborolane functionalities **11**

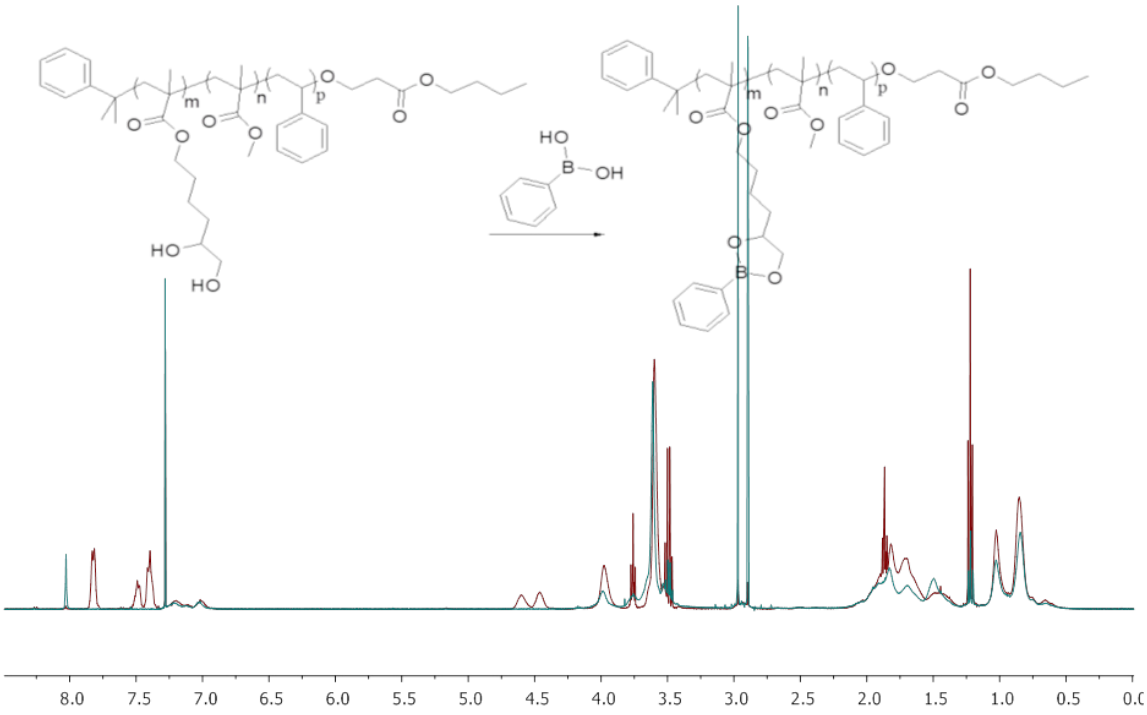

Fig S12
Comparison of ^{1}H-NMR spectra of PMMA with pending diols **10** (cyan) and PMMA with pending dioxaborolane functionalities **11** (burgundy) in $CDCl_3$

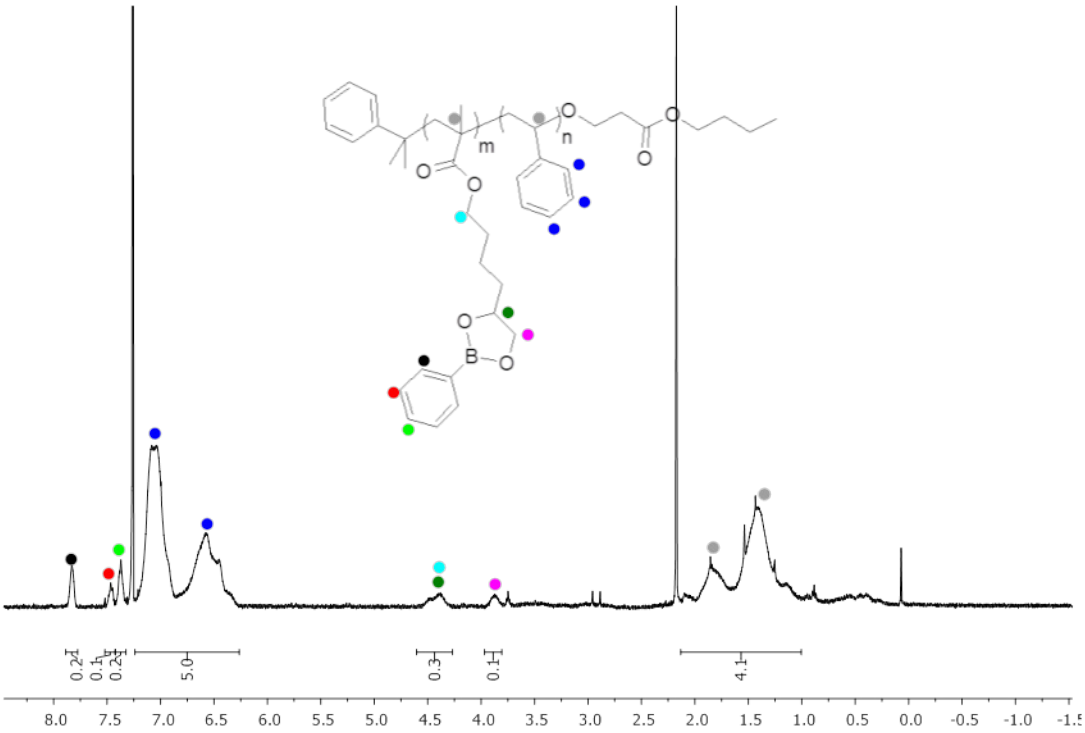

Fig S13
^{1}H-NMR spectrum of PS with pending dioxaborolanes **14** in $CDCl_3$

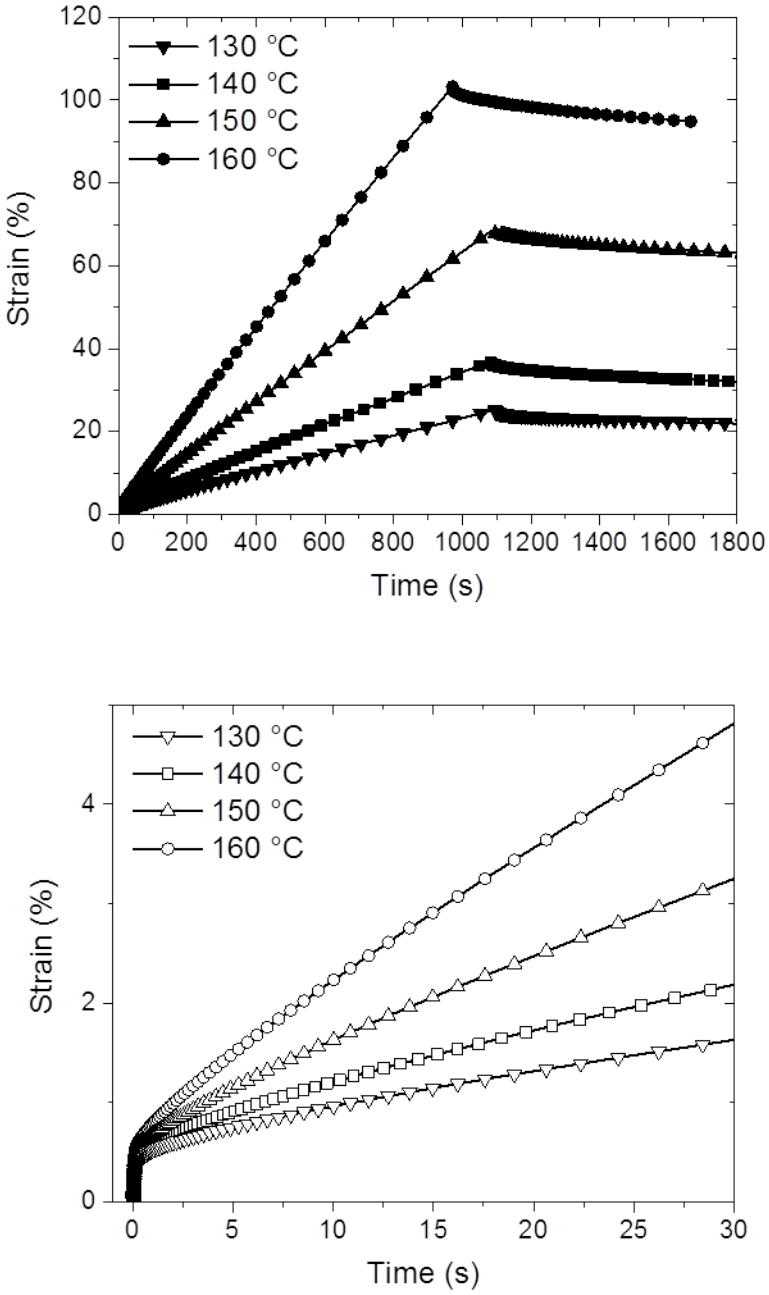

Fig. S14
Step-stress creep-recovery plots for PMMA vitrimer V1 at different temperatures (top) and zoom-in on the elastic region (bottom) (σ = 1000 Pa). Viscosities and relaxation times were extracted from fits on the linear regimes of the plots. 130 °C: $\eta = 4.6\ 10^6$ Pa.s and τ = 73 s. 140 °C: $\eta = 3.1\ 10^6$ Pa.s and τ = 69 s. 150 °C: $\eta = 1.6\ 10^6$ Pa.s and τ = 44 s. 160 °C: $\eta = 9.7\ 10^5$ Pa.s and τ = 34 s.

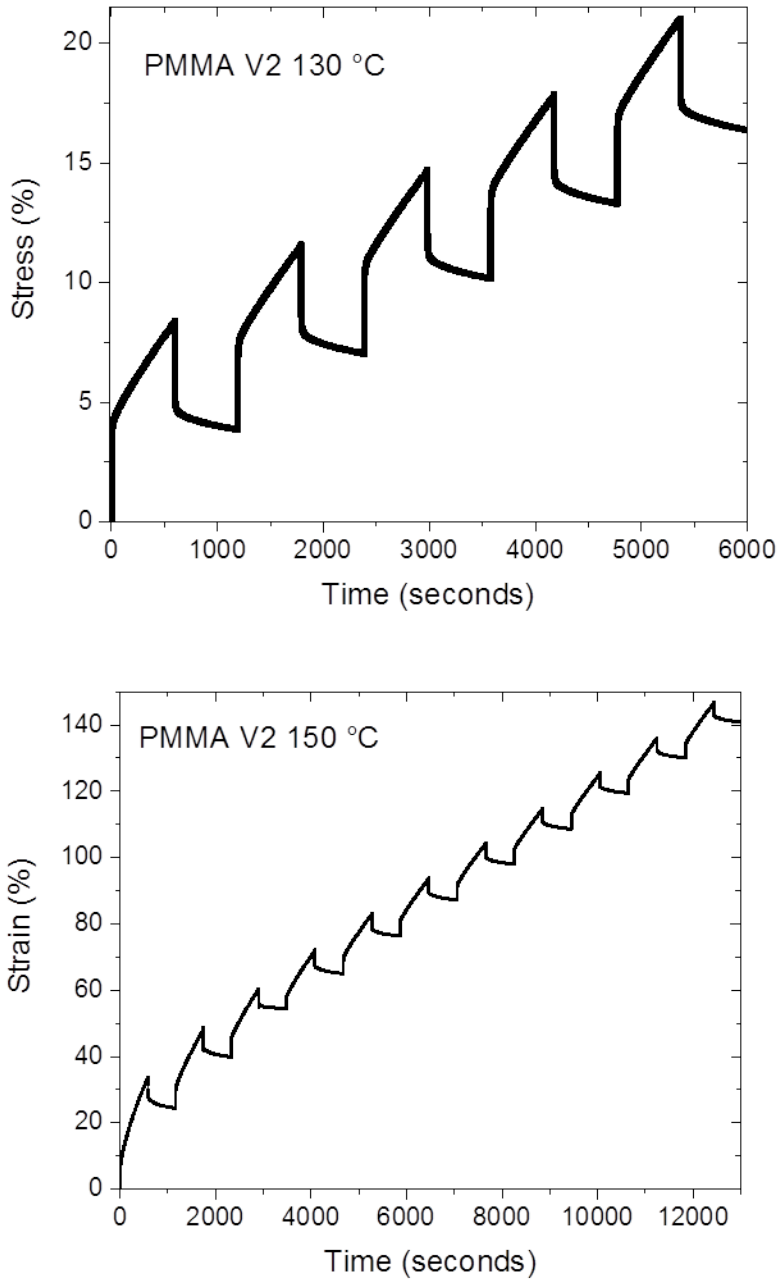

Fig. S15
Consecutive step-stress creep-recovery plots for PMMA vitrimer V2 at 130 °C (top) and 150 °C (bottom) (σ = 3500 Pa). Viscosities and relaxation times were extracted from fits on the linear regimes of the plots. 130 °C: $\eta = 5.6\ 10^7$ Pa.s and τ = 660 s. 150 °C: $\eta = 1.8\ 10^7$ Pa.s and τ = 352 s.

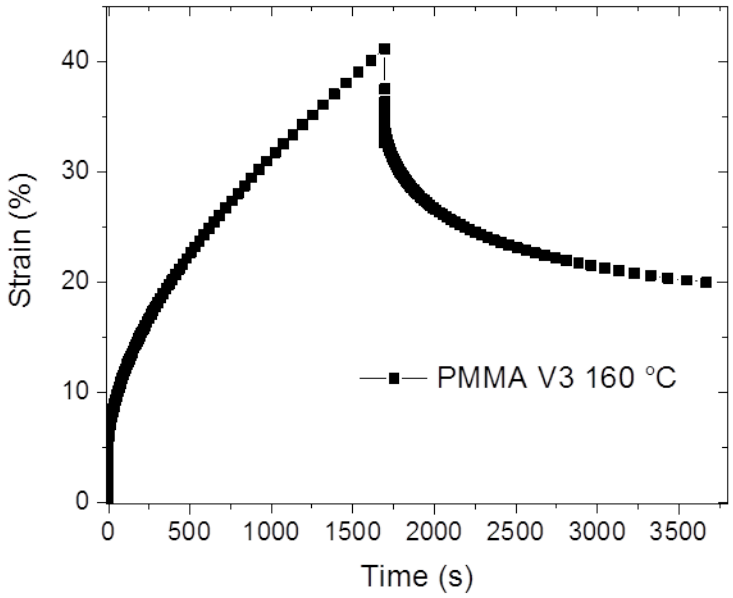

Fig. S16
Step-stress creep-recovery plots for PMMA vitrimer V3 at 160 °C (σ = 10000 Pa). The viscosities and relaxation times were extracted from a fit on the linear regime of the plot. $\eta = 7.2\ 10^7$ Pa.s and τ = 1270 s.

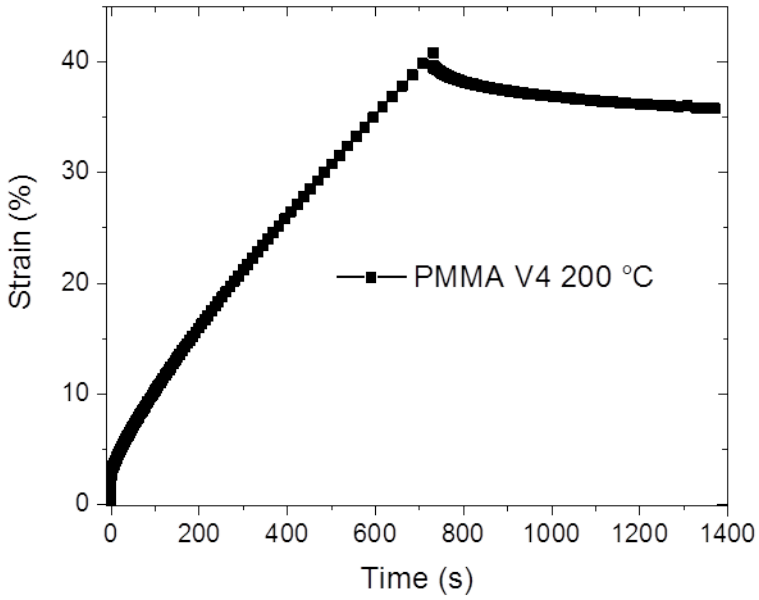

Fig. S17
Step-stress creep-recovery plots for PMMA vitrimer V4 at 200 °C (σ = 5000 Pa). The viscosity and relaxation time were extracted from a fit on the linear regime of the plot. $\eta = 1.1\ 10^7$ Pa.s and τ = 189 s.

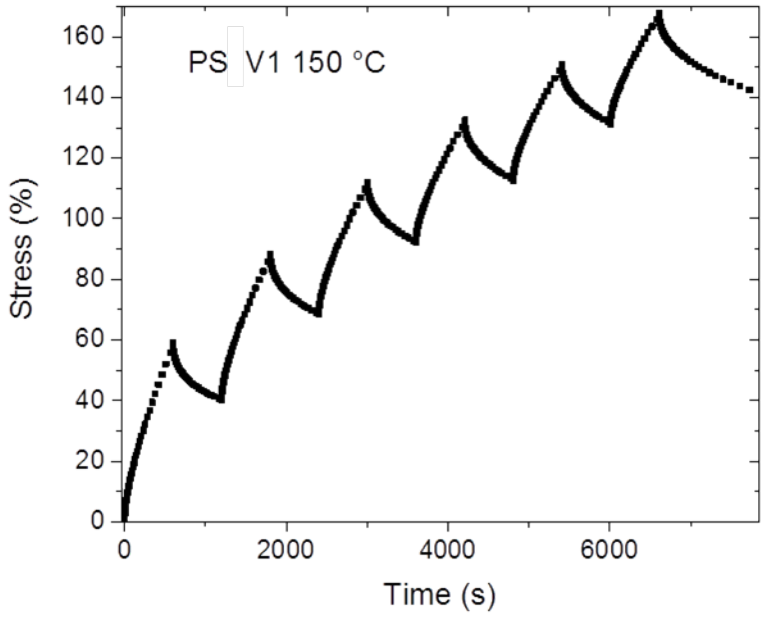

Fig. S18
Consecutive step-stress creep-recovery plots for PS vitrimer V1 at 150 °C (σ = 5000 Pa). The viscosity and relaxation time were extracted from a fit on the linear regime of the plot. $\eta = 5.8\ 10^6$ Pa.s and $\tau = 208$ s was extracted.

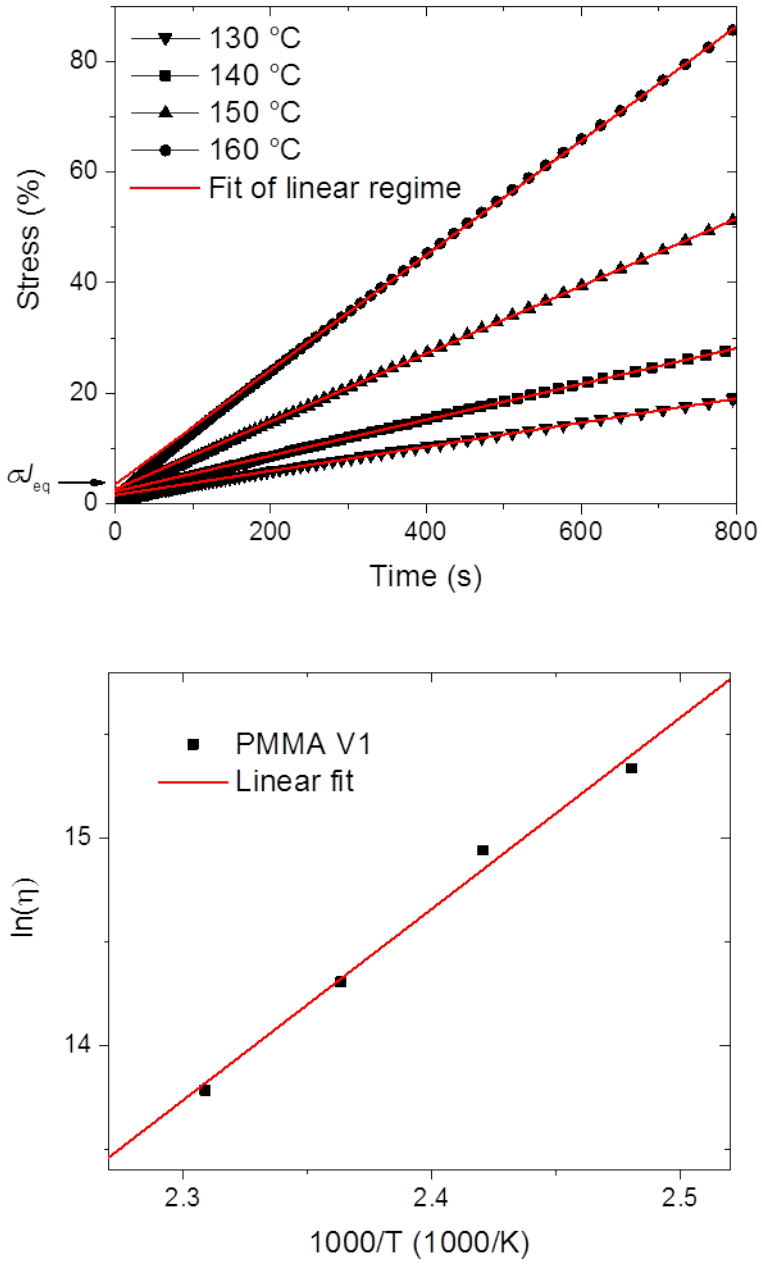

Fig. S19
Top: step-stress creep-recovery plots for PMMA vitrimer V1 at different temperatures and fits of their linear regimes to extract viscosities. Bottom: plot of ln(η) versus 1000/T and a linear fit to extract the activation energy E_a = 76.7±5.5 kJ/mol.

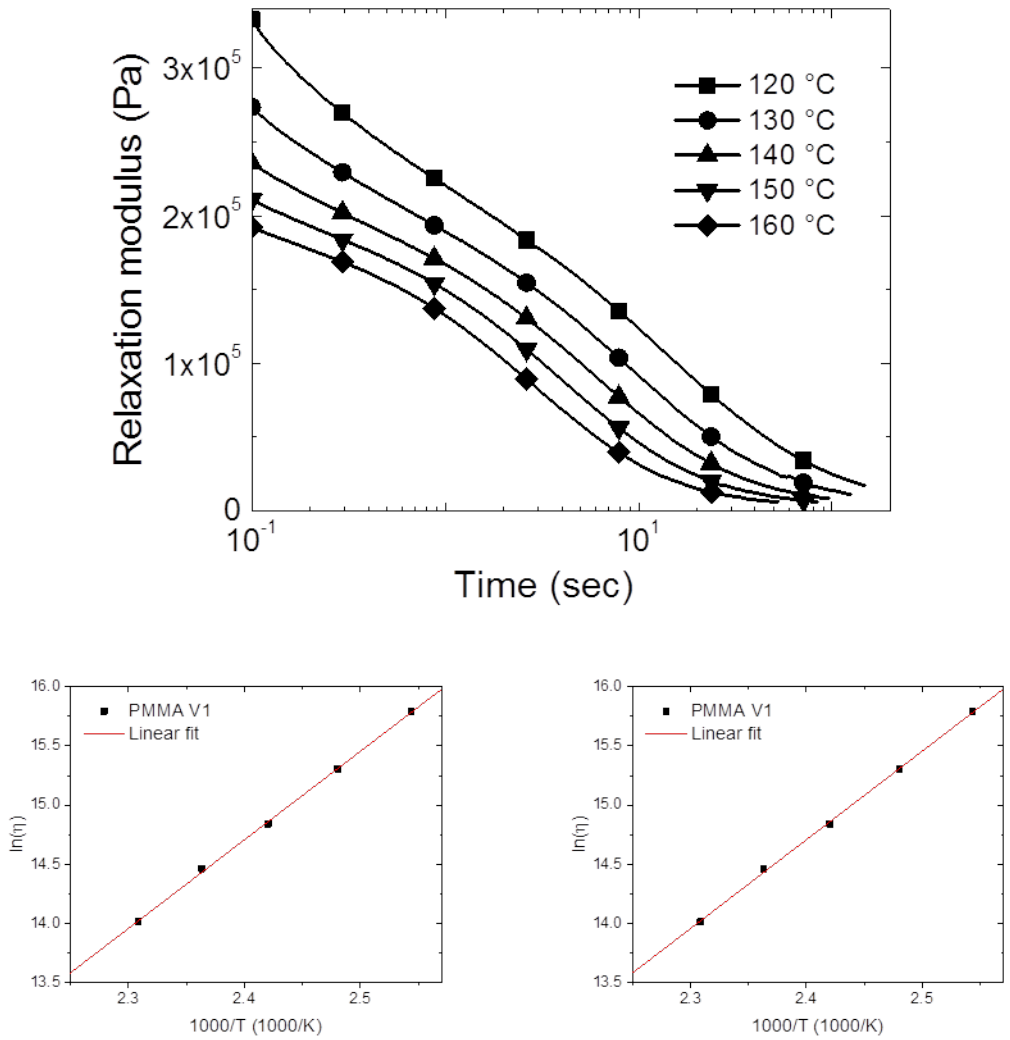

Fig. S20
Top: stress relaxation PMMA vitrimer V1 at different temperatures. Bottom: plot of ln(η) and ln(τ) versus 1000/T and linear fits to extract the activation energy on viscosity E_a = 62.3±1 kJ/mol and on relaxation time E_a = 43.2±3.8 kJ/mol. Viscosities were extracted from stress relaxation data with Equation S3. Relaxation times were extracted from stress relaxation data with Equation S4.

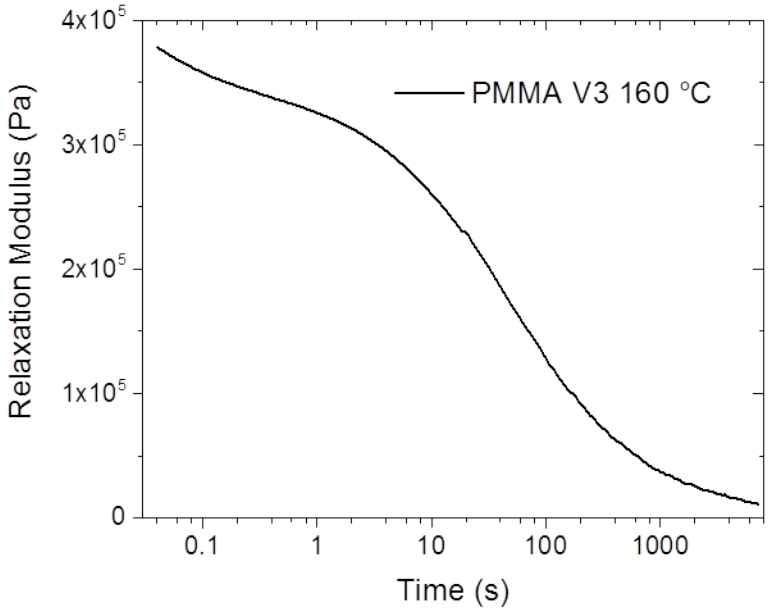

Fig. S21
Stress relaxation plot for PMMA vitrimer V3 at 160 °C during a step strain of 1%. The viscosity is 1.85 10^8 Pa.s at 160 °C.

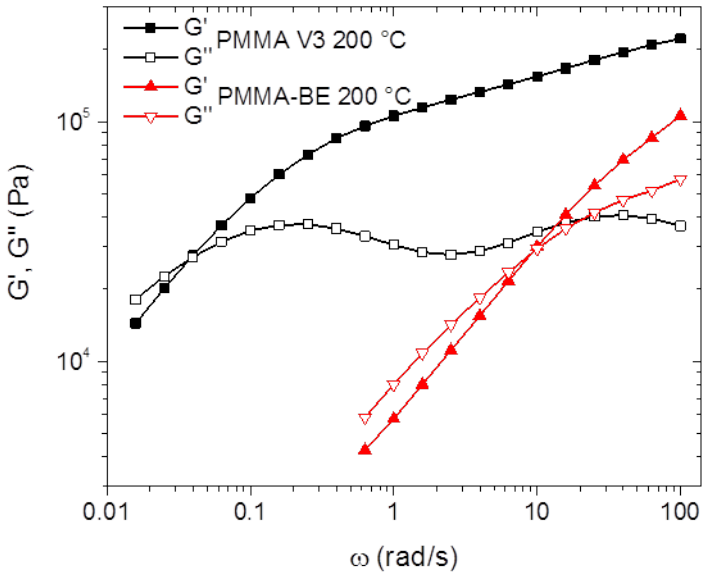

Fig. S22
Storage (G') and loss (G") moduli as a function of angular frequency (ω) for PMMA vitrimer V3 and its linear precursor bearing pending dioxaborolanes at 200 °C. Measurements were carried out at a fixed shear strain amplitude of 1%.

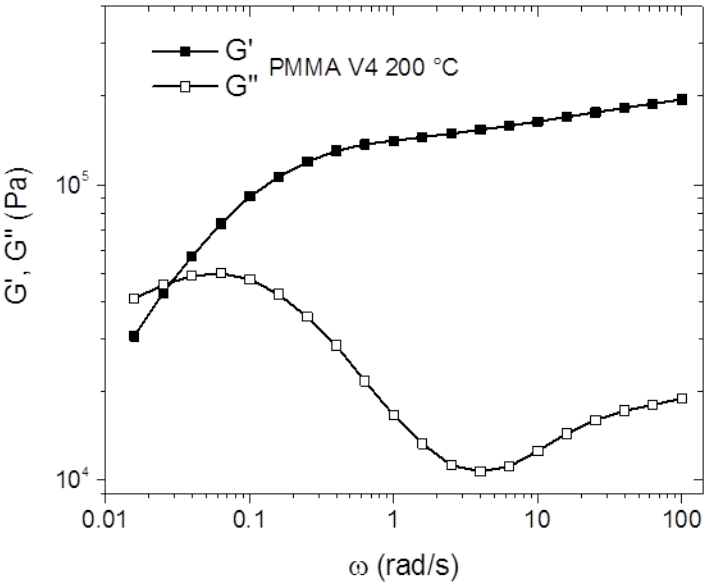

Fig. S23
Storage (G') and loss (G") moduli as a function of angular frequency (ω) for PMMA vitrimer V4 at 200 °C. Measurements were carried out at a fixed shear strain amplitude of 1%.

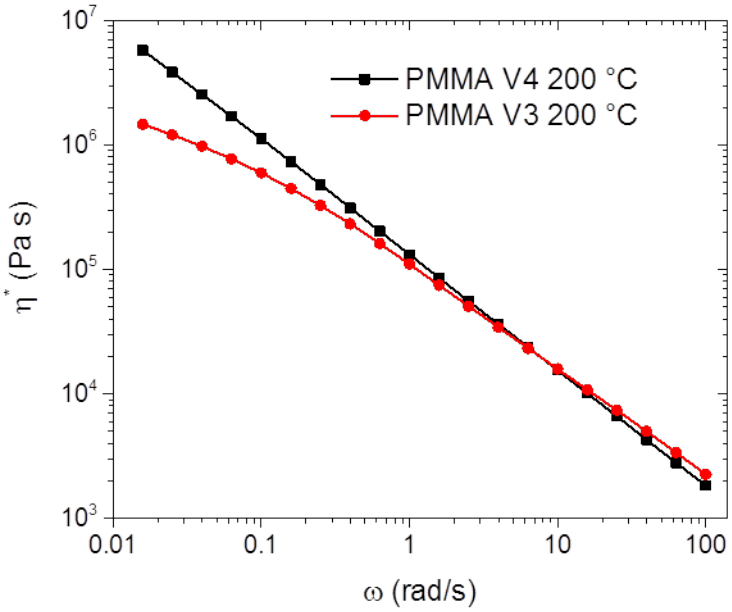

Fig. S24
Complex viscosities (|η∗|) as a function of angular frequency (ω) for PMMA vitrimers V3 and V4 at 200 °C. Measurements were carried out at a fixed shear strain amplitude of 1%. Complex viscosity at ω = 0.02 rad/s is |η∗| = 1.3 10^6 for PMMA V3 and |η∗| = 4.8 10^6 for PMMA V4.

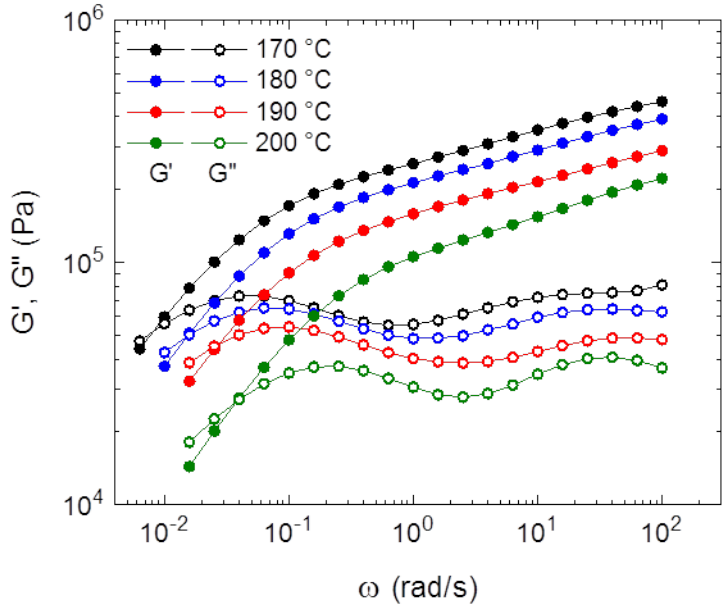

Fig. S25
Storage (G') and loss (G") moduli as a function of angular frequency (ω) for PMMA vitrimer V3 at 170, 180, 190 and 200 °C. Measurements were carried out at a fixed shear strain amplitude of 1%.

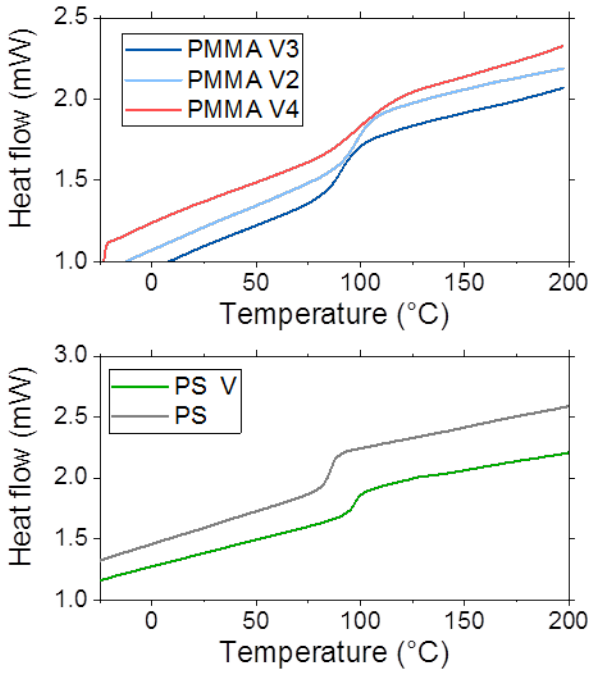

Fig. S26
Differential scanning calorimetry of PMMA vitrimers V2-V4 (top), PS V vitrimer and its linear precursor (bottom).

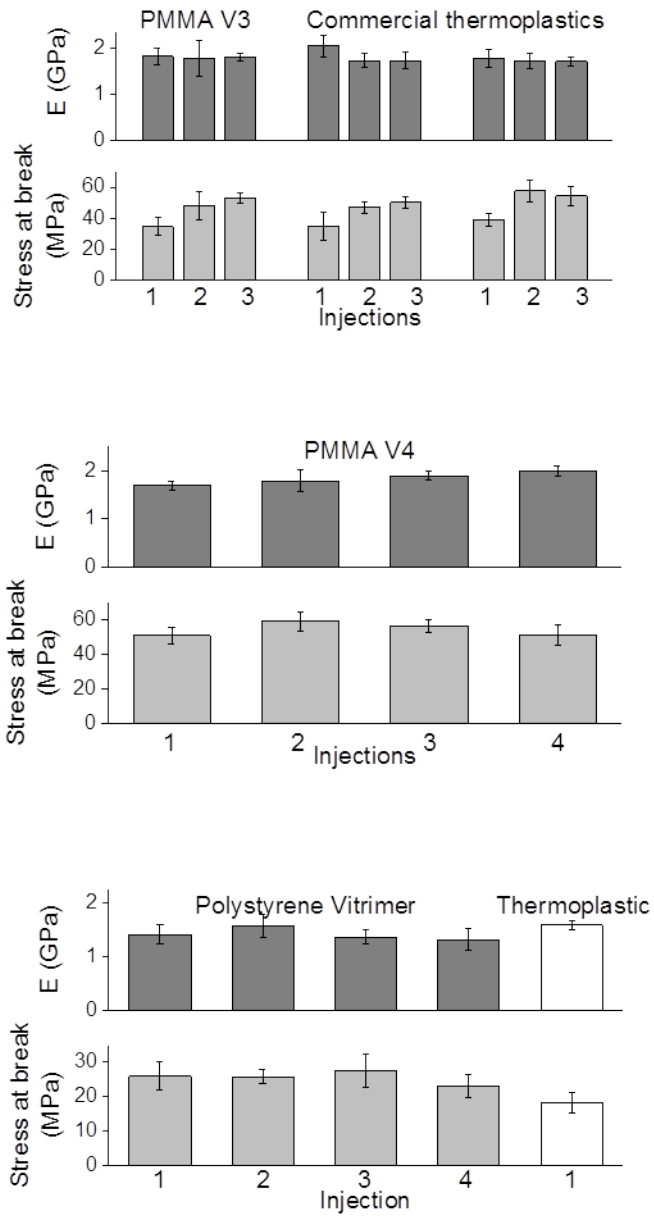

Fig. S27
Successive mechanical testing of PMMA and PS vitrimers after grinding of samples followed by injection molding. Top: PMMA vitrimer V3 and two commercially available thermoplastic PMMAs. Middle: PMMA vitrimer V4. Bottom: PS vitrimer V1 and its linear precursor. 1 corresponds to the first injection of the vitrimer as synthesized. For every injection experiment 3 to 5 specimens were tested.

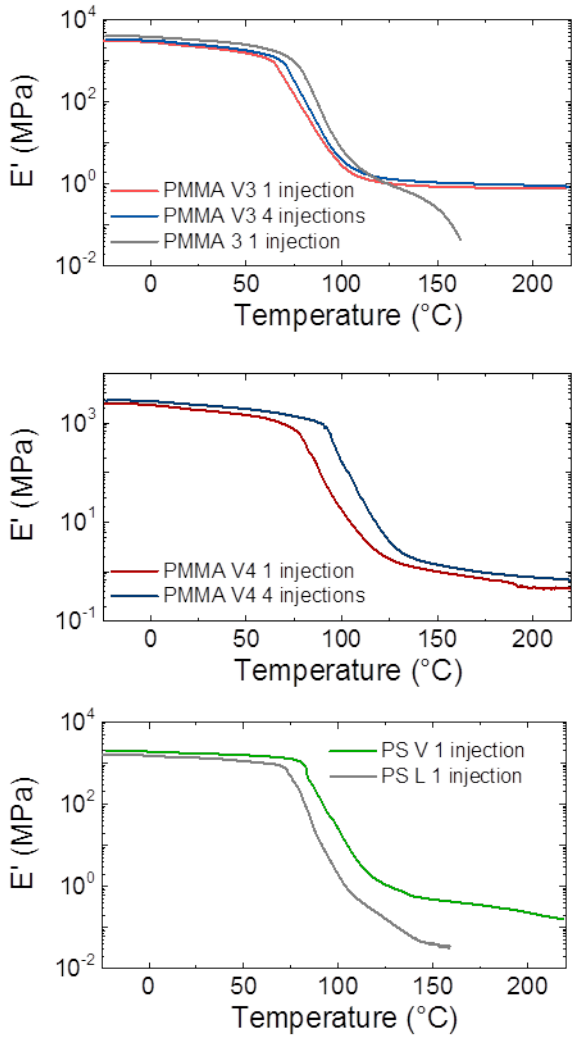

Fig. S28
Dynamic mechanical analysis of vitrimers and of their linear precursors during temperature ramp up at 3 °C/min and fixed frequency f = 1 Hz in tensile testing mode. From top to bottom: PMMA vitrimer V3 after 1 and 4 injections and its linear precursor after 1 injection; PMMA vitrimer V4 after 1 and 4 injections; PS vitrimer and its linear precursor after 1 injection.

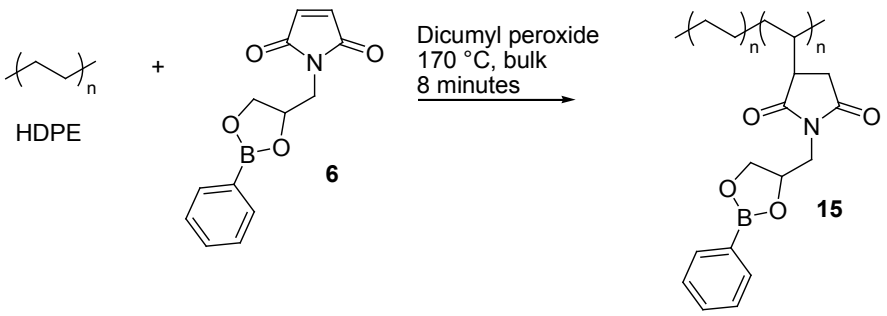

Fig S29
Synthesis of grafted HDPE with pending dioxaborolanes **15** by reactive extrusion.

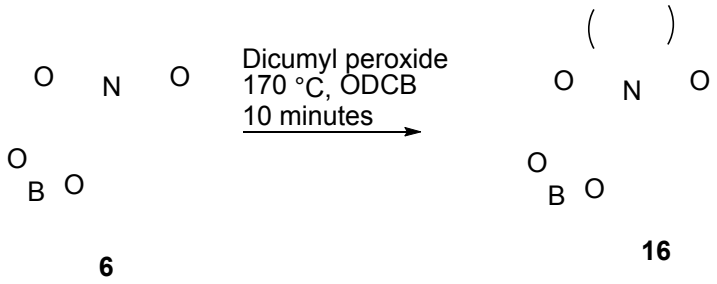

Fig S30
Synthesis of polymaleimide **16** with pending dioxaborolanes.

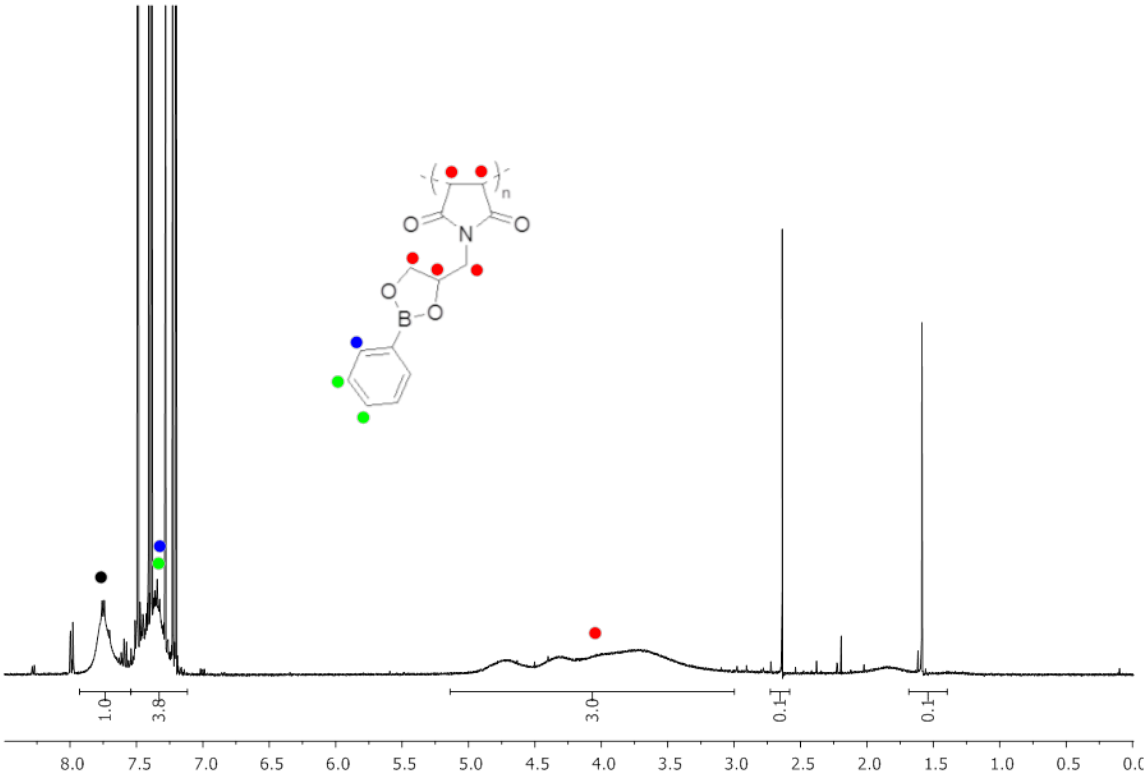

Fig S31
^{1}H-NMR spectrum of polymaleimide **16** in $CDCl_3$.

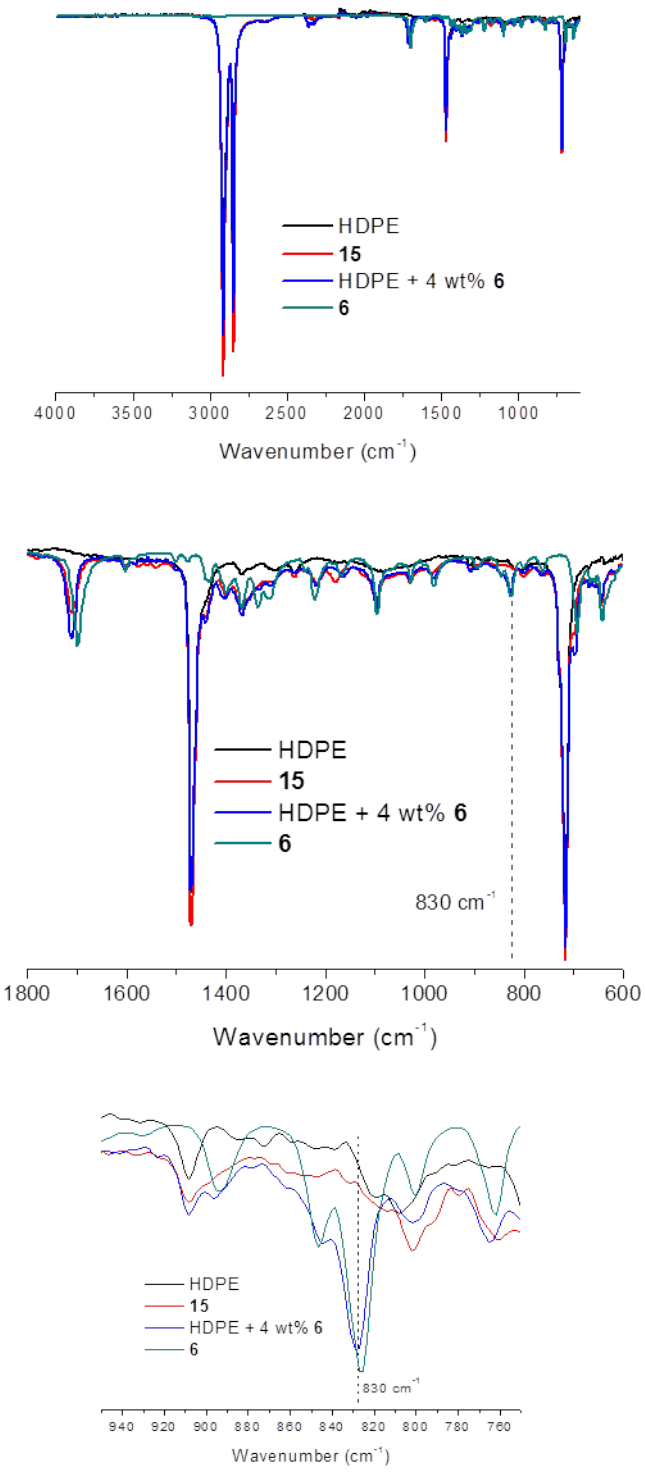

Fig. S32
Comparison of FT-IR spectra of HDPE, grafted HDPE **15**, a physical mixture of HDPE and **6** and maleimide **6**.

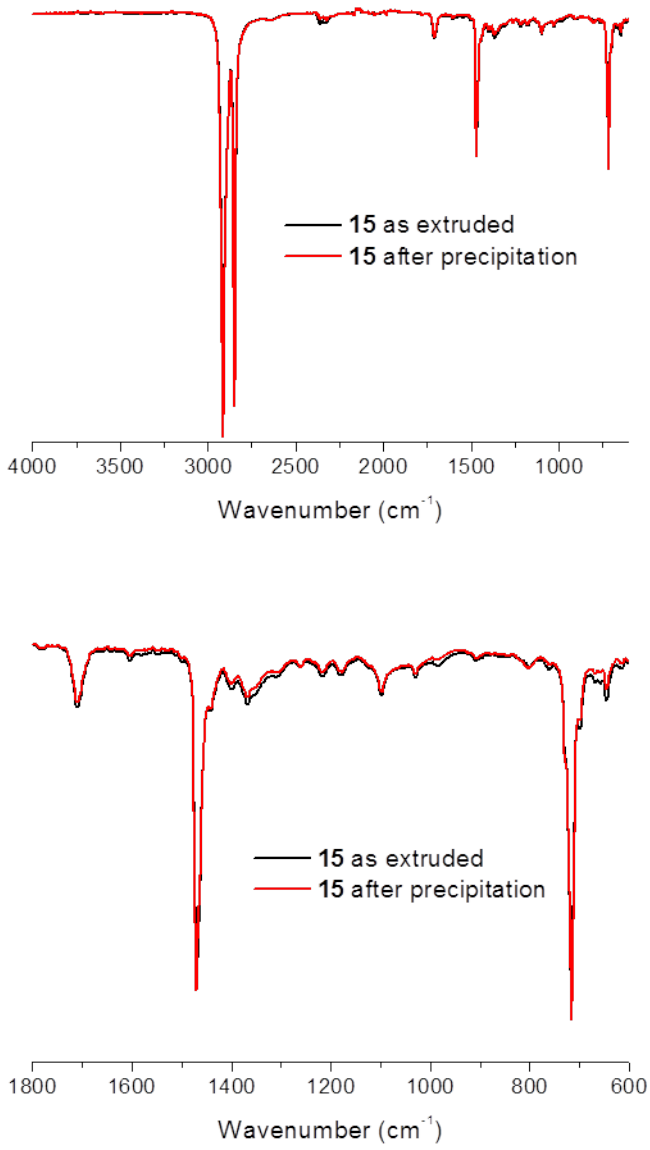

Fig. S33
Comparison of FT-IR spectra of extruded and precipitated HDPE grafted with pending dioxaborolanes **15.**

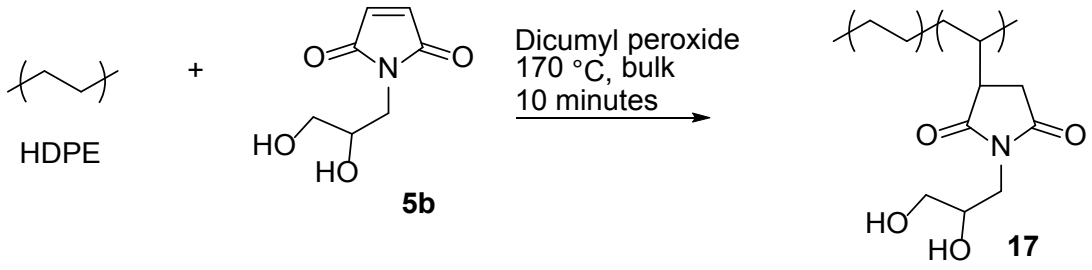

Fig S34
Synthesis of grafted HDPE with pending diols **17** by reactive extrusion.

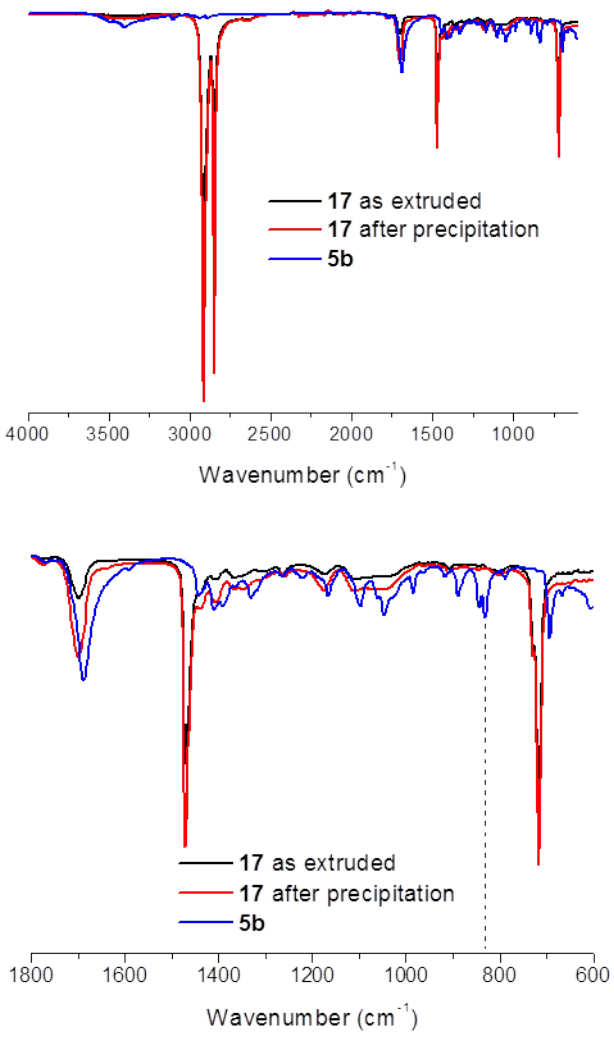

Fig. S35
Comparison of FT-IR spectra of extruded and precipitated HDPE grafted with pending diols **17** and diol-maleimide **5b.**

Fig. S36
Digital pictures of extrudates at the die exit: HDPE vitrimer based on BE maleimide (left) and diol maleimide grafted HDPE with crosslinker (right). The processing conditions are the same in both cases (the barrel temperature is 170 °C).

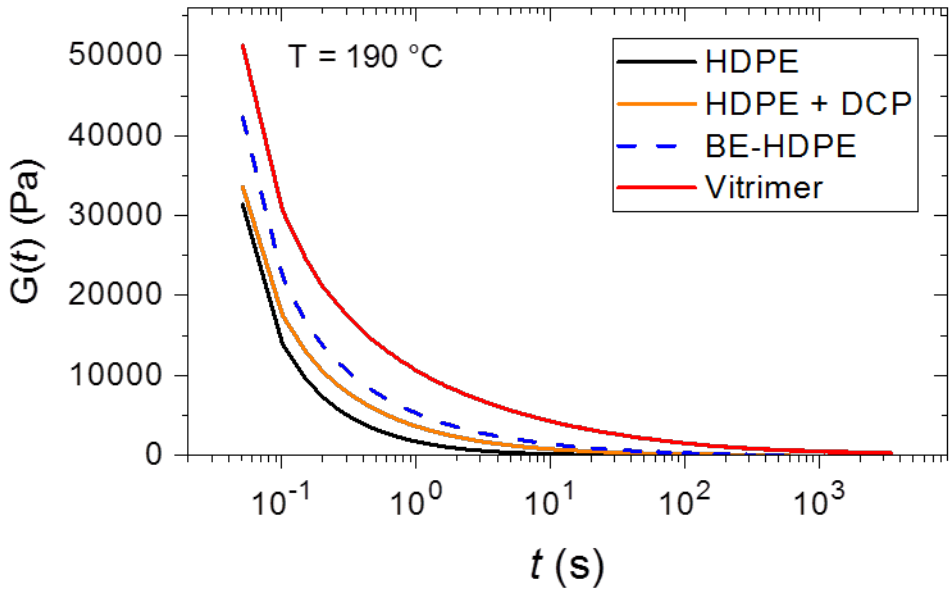

Fig. S37
Stress relaxation plots at 190 °C for HDPE (black), HDPE + 0.05 wt% DCP (orange), 4 wt% grafted BE-HDPE **15** (dashed blue) and HDPE vitrimer (red) during a step strain of 1% The viscosities η_0 were calculated from these data and according to equations S5. For HDPE, η_0 = 1.2 10^4 Pa.s, for HDPE + 0.05 wt% DCP, η_0 = 7.18 10^4 Pa.s, for 4 wt% grafted BE-HDPE **15**, η_0 = 1.26 10^5 Pa.s, for HDPE vitrimer, η_0 = 1.78 10^6 Pa.s.

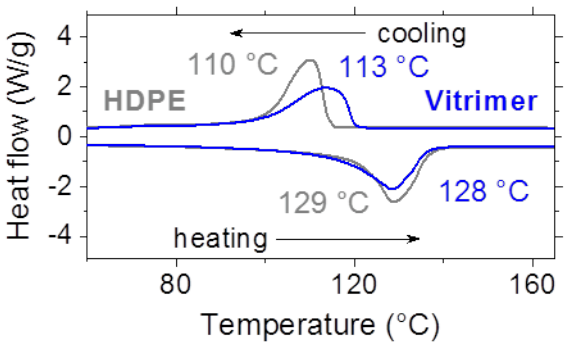

Fig. S38
Differential scanning calorimetry of HDPE vitrimer and its precursor. The degree of crystallinity is 59.9% for HDPE and 56.2% for the HDPE vitrimer, based on the specific enthalpy of melting.

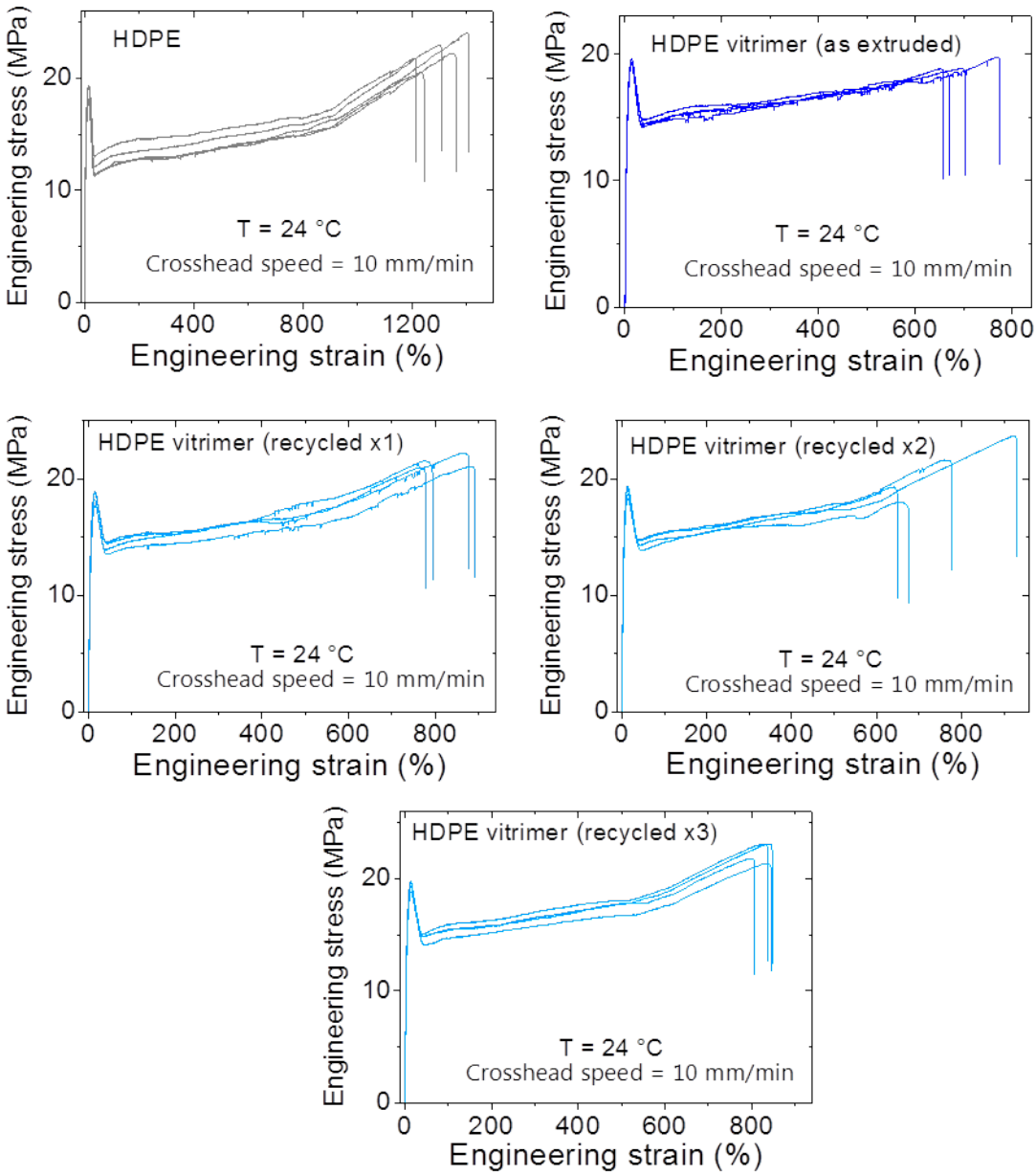

Fig. S39
Tensile stress-strain curves at 24 °C for the starting HDPE and the as processed and recycled (up to 3 times) HDPE vitrimer. Results on multiple specimens (N = 5 specimens tested for HDPE and N = 4 specimens tested for HDPE vitrimer in all cycles of recycling) are shown for reproducibility.

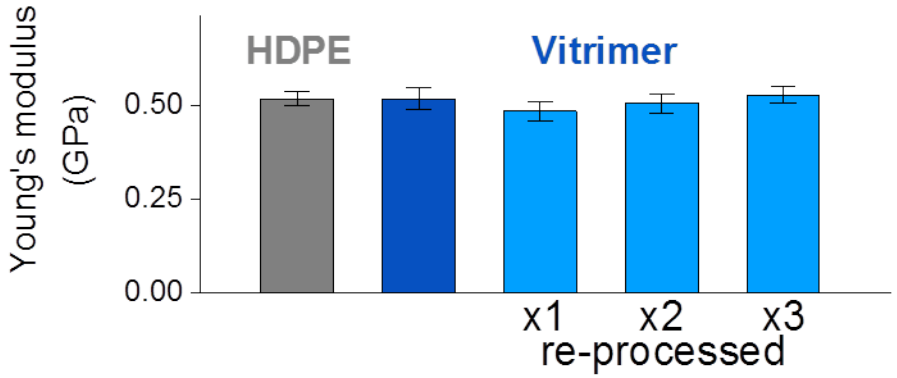

Fig. S40
Young's modulus for the starting HDPE and the as processed and recycled (up to 3 times) HDPE vitrimer at T = 24 °C. For HDPE N = 5 specimens tested and for HDPE vitrimer N = 4 specimen tested in all cycles of recycling.

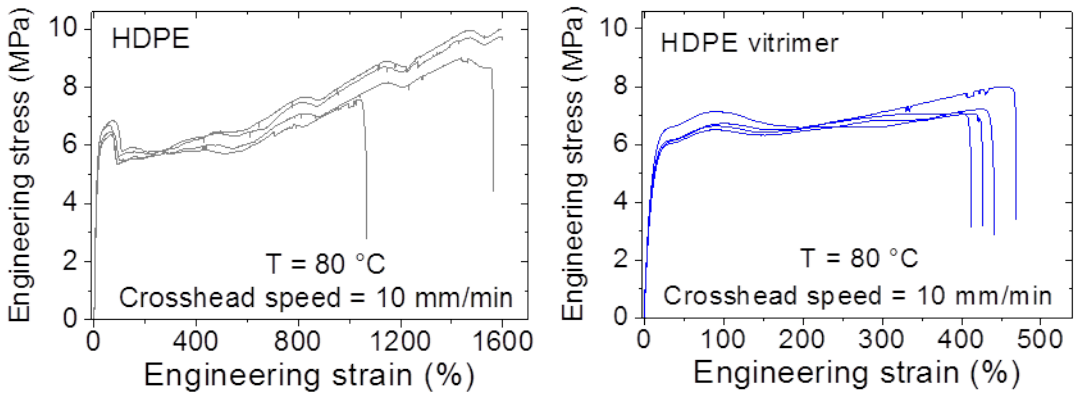

Fig. S41
Tensile stress-strain curves at 80 °C for the starting HDPE (left) and the HDPE vitrimer (right). Results on multiple specimens (N = 4 specimens tested for both HDPE and HDPE vitrimer) are shown for reproducibility.

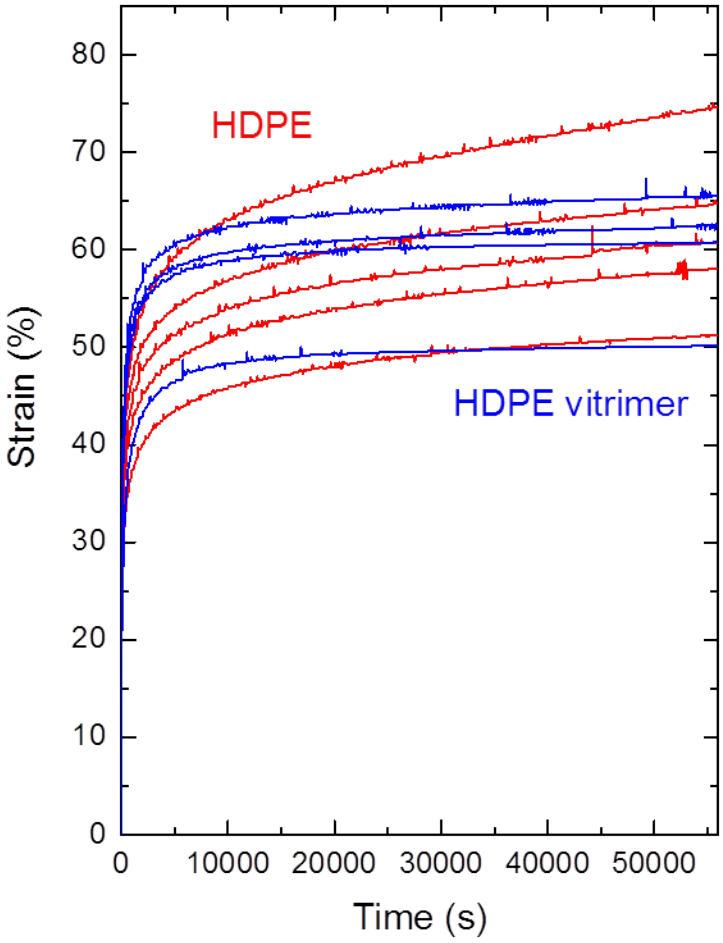

Fig. S42
Elongational creep tests at 80 °C and 5 MPa for the starting HDPE (in red) and the HDPE vitrimer (in blue). Results on multiple specimens (N = 5 specimens tested for HDPE and N = 4 specimens tested for HDPE vitrimer) are shown for reproducibility.

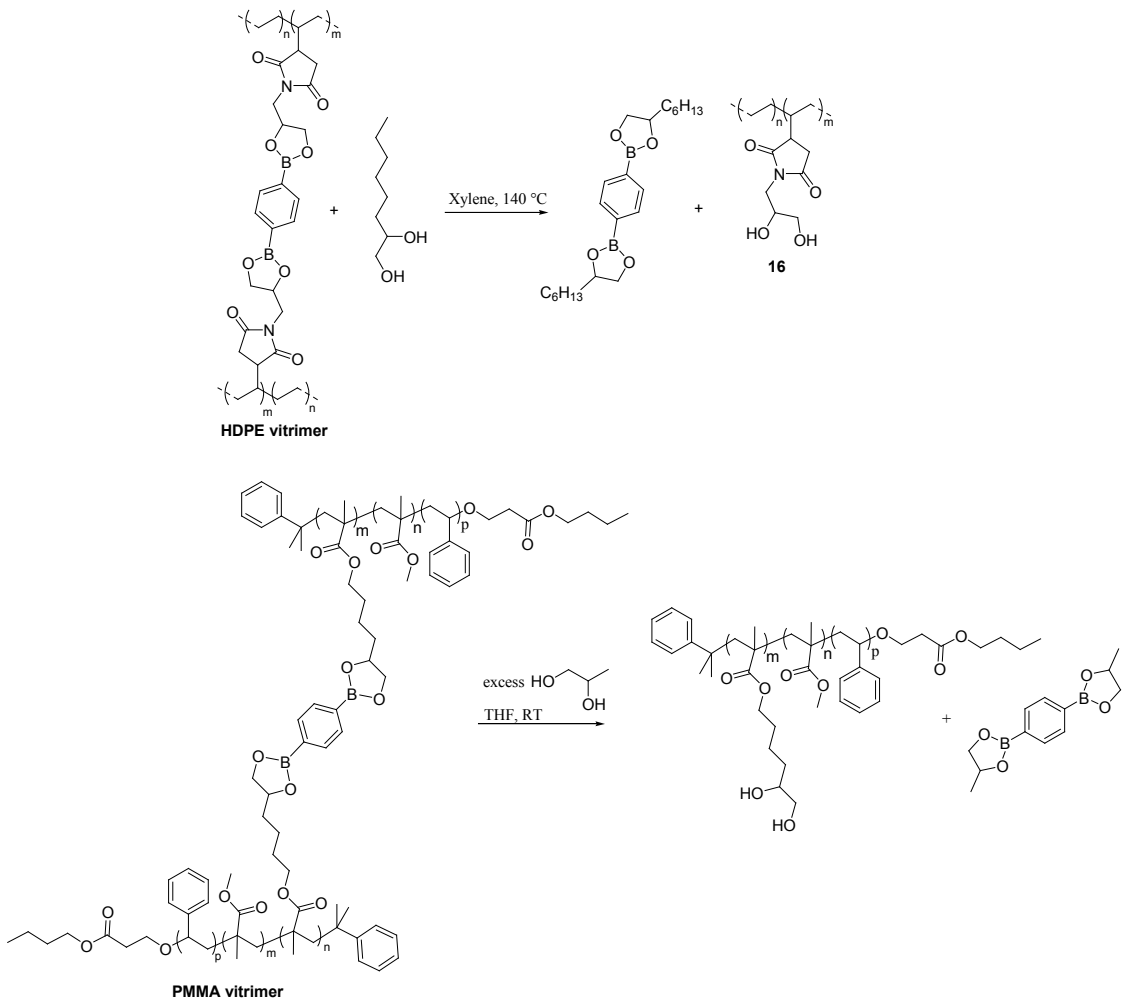

Fig S43

Diolysis of dioxaborolane bonds in HDPE and PMMA vitrimers with 1,2-octanediol and 1,2-propanediol, respectively, to yield soluble, linear polymers with pending diol functionalities.

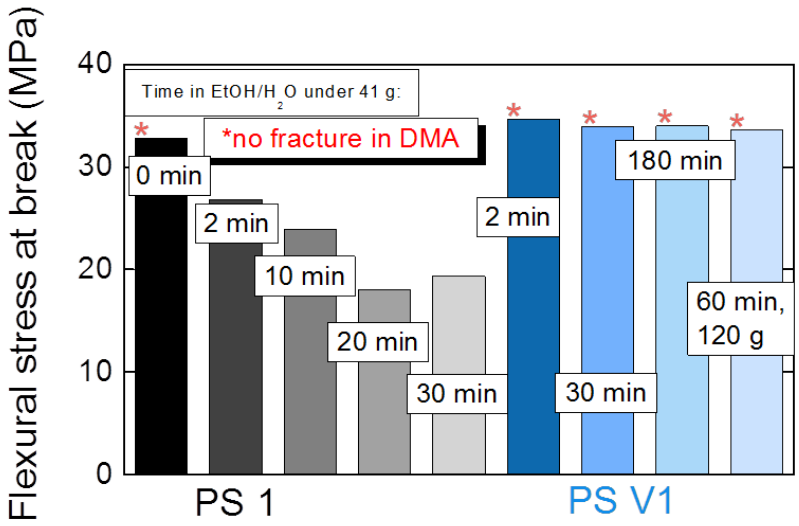

Fig. S44
Environmental stress cracking experiments of PS vitrimer V1 and of its linear thermoplastic precursor.

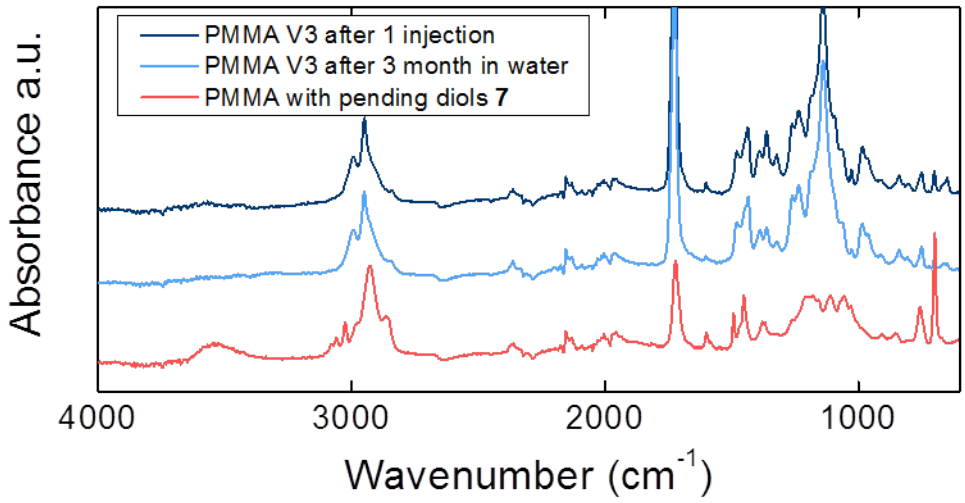

Fig. S45
FT-IR spectra of PMMA with pending diols, **7**, PMMA vitrimer V3 after one injection and after injection and immersion in water at room temperature for 3 months.

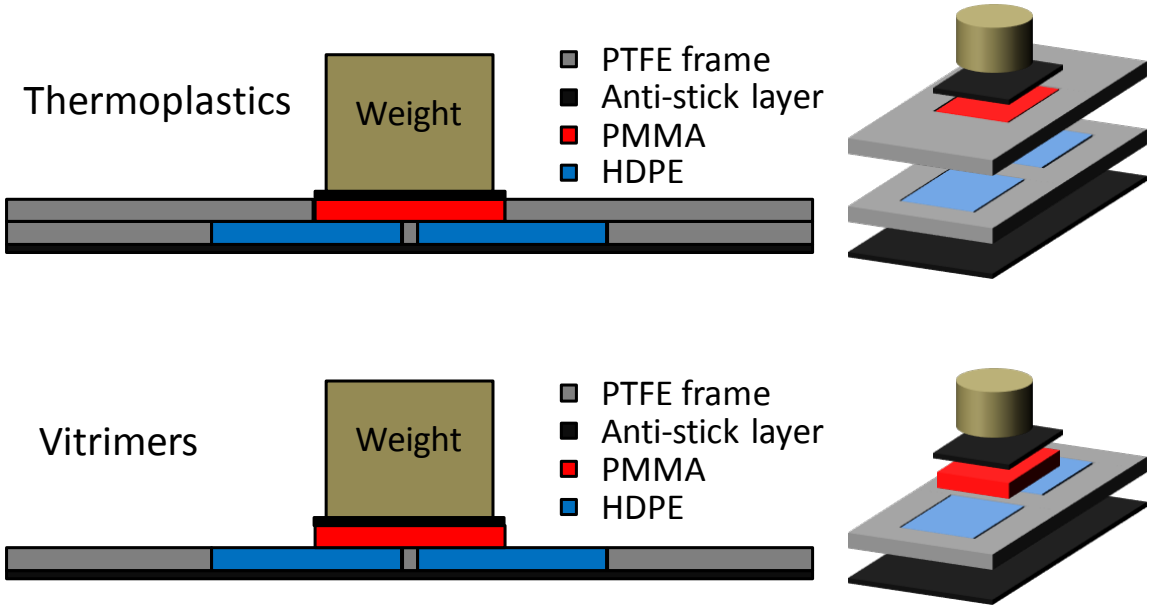

Fig. S46
Schematic of lap joints preparation set-ups. Top: set-up for thermoplastics. Bottom: set-up for vitrimers.

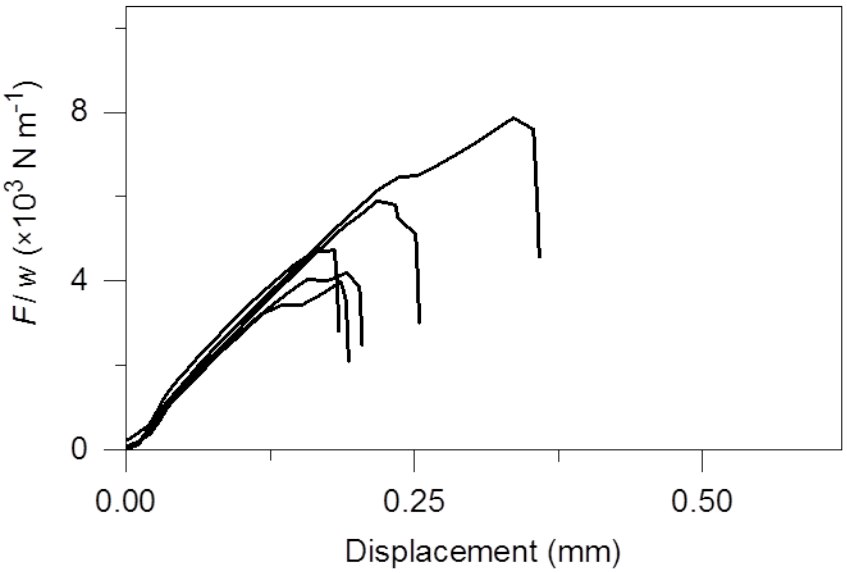

Fig. S47
Lap-shear test curves for HDPE-BE/PMMA-BE thermoplastics (BE grafted HDPE **15** and BE functionalized PMMA **8a**, respectively) lap joints prepared at 190 °C for 10 min. Crosshead speed is 10 mm/min. Results on multiple specimens (N = 5 specimens tested) are shown for reproducibility. The lap joints all broke by interfacial detachment. The adhesion energy was calculated to be 15 ± 6 $J.m^{-2}$.

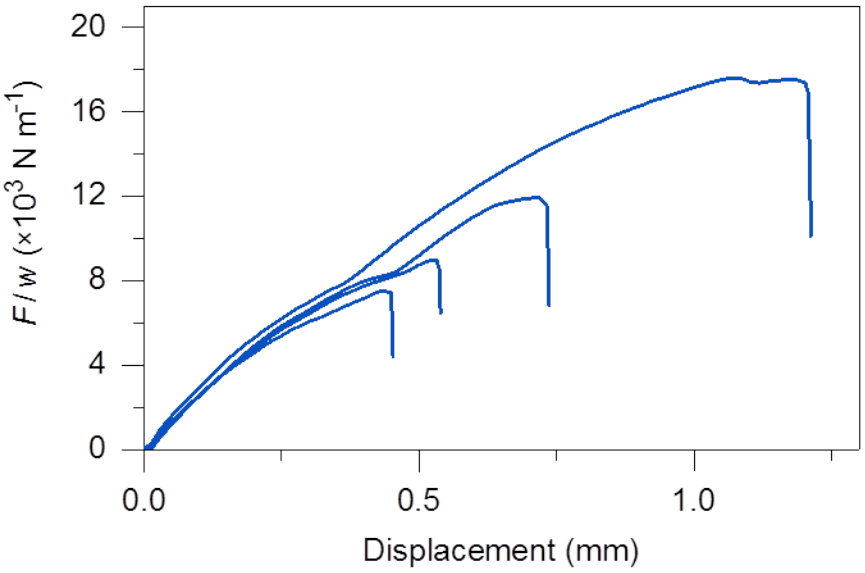

Fig. S48
Lap-shear test curves for HDPE vitrimer and PMMA vitrimer V5 lap joints prepared at 190 °C for 10 min. Crosshead speed is 10 mm/min. Results on multiple specimens (N = 4 specimens tested) are shown for reproducibility. The lap joints all broke by interfacial detachment. The adhesion energy was calculated to be 68 ± 37 $J.m^{-2}$.

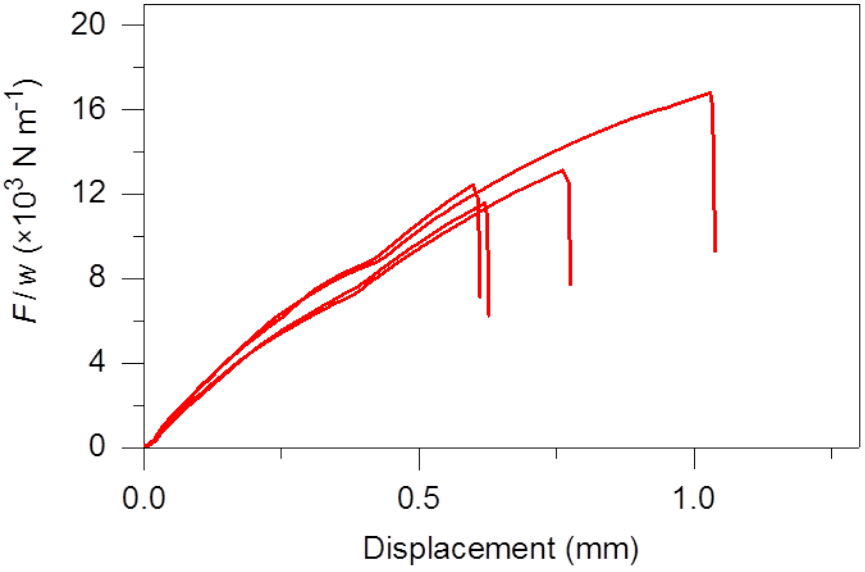

Fig. S49
Lap-shear test curves for HDPE vitrimer and PMMA vitrimer V5 lap joints prepared at 190 °C for 20 min. Crosshead speed is 10 mm/min. Results on multiple specimens (N = 4 specimens tested) are shown for reproducibility. The lap joints all broke via bulk fracture within the PMMA vitrimer layer.

Tables S1-S12

Table S1: Solubility analysis on PMMA thermoplastics **10** and **11,** PMMA vitrimer V5, and PMMA-diol network V5 after TGA experiments

Polymer, vitrimer, or network	Time (min)	Temperature (°C)	Sample weight (mg)	Gel content (mg)	Gel content (%)
10	5	200	7.4	7.2	97.3
10	10	200	6.7	6.6	98.5
11	5	200	6.6	0	0
11	10	200	6.0	0	0
PMMA V5	5	200	11.5	0	0
PMMA V5	10	200	10.8	0	0
PMMA V5	30	150	12.1	0	0
PMMA-diol V5	5	200	15.4	10.9	70.8
PMMA-diol V5	10	200	13.6	12.3	90.4
PMMA-diol V5	30	150	12.8	9.5	74.2

Table S2

^{1}H-NMR integration data of diluted 1,2-butanediol (**D_2**) solutions (0.5 mL $CDCl_3$)

#	c_{D2} (mM)	Chemical shift (ppm)						
		Styrene (internal standard)		1,2-butanediol **(D_2)**				
		6.72	5.75	3.67 (CH_2)	3.44 (CH)	1.99 (CH)	1.81 (CH)	0.97 (CH_3)
1	25.5	1	1.03	2.31	1.21	1.1	1.12	3.51
2	10	1	1.02	0.79	0.42	0.38	0.37	1.15
3	5	1	1.03	0.39	0.21	0.19	0.19	0.55
4	1	1	1.03	0.13	0.07	0.06	0.06	0.15
5	0.5	1	1.03	0.1	0.06	0.05	0.05	0.09
6	0.1	1	1.03	nd*	nd*	nd*	nd*	0.03
*nd = not detectable								

Table S3
Poly(methyl methacrylate) vitrimers.

System	Poly(methyl methacrylates) with pending dioxaborolanes **8a**				Cross-linker 4 wt%
	M_n (kg/mol)	M_w (kg/mol)	$Đ$	MMA/dioxaborolane	
PMMA V1	22	26	1.18	3.3/1	2.2
PMMA V2	86	120	1.40	3.3/1	1.0
PMMA V3	86	120	1.40	3.3/1	2.2
PMMA V4	76	100	1.32	24/1	2.2
PMMA V5[a]	85	102	1.2	3.8/1	2.2

a) PMMA V5 is based on polymer **11** containing 5 mol% styrene.

Table S4
Polystyrene vitrimer

System	Polystyrene with pending dioxaborolanes **11**				Cross-linker 4 wt%
	M_n (kg/mol)	M_w (kg/mol)	$Đ$	Styrene/boronic ester	
PS V1	76	130	1.71	8.5/1	2.2

Table S5
Swelling experiments of PMMA V3 samples in THF (10 mL) for 24 hours after different cycles of reprocessing.

Sample	Injections	Mass dry (mg)	Mass swollen (mg)	Swelling ratio	Mass dried (mg)	Soluble fraction (%)
1	1	356	1979	4.7	350	1.7
2	1	256	1562	5.4	245	4.3
3	3	240	1430	5.0	239	0.4
4	3	198	1149	4.8	197	0.5

Table S6
Swelling experiments of PMMA V4 samples in THF (10 mL) for 72 hours after different cycles of reprocessing

Sample	Injections	Mass dry (mg)	Mass swollen (mg)	Swelling ratio	Mass dried (mg)	Soluble fraction (%)
1	1	130	680	4.2	130	0
2	1	106	589	4.6	105	0.9
3	1	99	636	5.6	97	2.0
4	4	142	710	4.0	141	0.7
5	4	202	1206	5.0	200	1.0
6	4	216	1210	4.6	216	0

Table S7
Swelling experiments of PS V1 samples in DCM (6 mL) after crosslinking in extrusion

Sample	Extrusions	Mass dry (mg)	Mass swollen (mg)	Swelling ratio	Mass dried (mg)	Soluble fraction (%)
1	2	81.5	2131	27.0	76	6.7
2	2	184	3874	21.7	171	7.0
3	2	151	3610	23.1	150	0.7

Table S8
Gel content and MFI of HDPE based materials.

Sample	Gel content (%)	Gel content after diolysis (%)	MFI (g/10 min) 190 °C, 2.16 kg	MFI (g/10 min) 190 °C, 10 kg
HDPE	0	-	1.9 ± 0.03 (N = 10)	-
HDPE + 0.05 wt% DCP	0	-	-	-
4 wt% BE-HDPE	0	-	-	12.1 ± 0.60 (N = 5)
Vitrimer (4 wt% BE-HDPE + 4 wt% crosslinker)	31.7 ± 3.2 (N = 3)	0	-	3.7 ± 0.09 (N = 10)
4 wt% D-HDPE	0	-	-	-
4 wt% D-HDPE + 4 wt% crosslinker	0	-	-	-

Table S9
GPC results of linear precursors and PMMA vitrimers V3 and V4 cleaved by transesterification after reprocessing by injection molding and PS vitrimer V1 after extrusion.

#	M_n (g/mol)	M_w (g/mol)	$Đ$	Processing
PMMA V3				
Parent **7**	71 000	96 000	1.35	-
Parent **8a**	86 000	120 000	1.40	-
Cleaved Vitrimer	75 000	105 000	1.40	1 inj.
Cleaved Vitrimer	76 000	108 000	1.42	3 inj.
PMMA V4				
Parent **7**	65 000	80 000	1.23	-
Parent **8a**	69 000	84 000	1.22	-
Cleaved Vitrimer	75 000	97 000	1.29	1 inj.
Cleaved Vitrimer	76 000	101 000	1.33	4 inj.
PS V1				
Parent **12**	75 000	118 000	1.57	-
Parent **13**	77 000	123 000	1.60	-
Parent **14**	76 000	130 000	1.71	-
Cleaved Vitrimer	76 000	129 000	1.70	2 extr.

Table S10

Water uptake results on PMMA V5. At room temperature the average water uptake is 2.0±0.9 wt%. The average gel content after swelling in THF is 89.9±5.5%.

Sample	Initial weight (mg)	Weight after water uptake (mg)	Weight gain (mg)	Water uptake (%)	Weight after drying 2 days (mg)	Mass of dried gel (mg)	Gel content (%)
1	100.1	101.6	1.5	1.5	100.6	82.7	82.6
2	95.6	98.9	3.3	3.6	98.5	84.9	88.8
3	95.3	97.4	2.1	2.2	97.1	91.5	96
4	99.4	100.9	1.5	1.5	100.9	94.1	94.7
5	100.9	102.2	1.3	1.3	102.2	88.1	87.3

Table S11

Water uptake results on PMMA-diol V5. At room temperature the average water uptake is 9.5±1.2 wt%. The average gel content after swelling in THF is 19.0±4.9%

Sample	Initial weight (mg)	Weight after water uptake (mg)	Weight gain (mg)	Water uptake (%)	Weight after drying 2 days (mg)	Mass of dried gel (mg)	Gel content (%)
1	97.4	105.8	8.4	8.6	99.2	19.6	20.1
2	90.9	98	7.1	7.8	91	20.6	22.7
3	94.4	104.1	9.7	10.3	95.8	11.5	12.2
4	98.8	108.8	10	10.1	100.9	15.7	15.9
5	76.2	84.2	8	10.5	77.5	18.3	24.0

Table S12

Water uptake results on PMMA. At room temperature the average water uptake is 1.8±0.9 wt%. No gel was observed after swelling in THF.

Sample	Initial weight (mg)	Weight after water uptake (mg)	Weight gain (mg)	Water uptake (%)	Weight after drying 2 days (mg)	Mass of dried gel (mg)
1	107	110.6	3.6	3.4	109.3	0
2	111.9	113.7	1.8	1.6	112.2	0
3	112.9	114.9	2	1.8	113.5	0
4	84.3	85.5	1.2	1.4	84	0
5	101.9	102.9	1	1.0	101.5	0

References and Notes

1. D. Montarnal, M. Capelot, F. Tournilhac, L. Leibler, Silica-like malleable materials from permanent organic networks. *Science* **334**, 965–968 (2011). doi:10.1126/science.1212648 Medline

2. M. Capelot, M. M. Unterlass, F. Tournilhac, L. Leibler, Catalytic control of the vitrimer glass transition. *ACS Macro Lett.* **1**, 789–792 (2012). doi:10.1021/mz300239f

3. J. P. Brutman, P. A. Delgado, M. A. Hillmyer, Polylactide vitrimers. *ACS Macro Lett.* **3**, 607–610 (2014). doi:10.1021/mz500269w

4. W. Denissen, G. Rivero, R. Nicolaÿ, L. Leibler, J. M. Winne, F. E. Du Prez, Vinylogous urethane vitrimers. *Adv. Funct. Mater.* **25**, 2451–2457 (2015). doi:10.1002/adfm.201404553

5. W. Denissen, J. M. Winne, F. E. Du Prez, Vitrimers: Permanent organic networks with glass-like fluidity. *Chem. Sci. (Camb.)* **7**, 30–38 (2016). doi:10.1039/C5SC02223A

7. D. J. Fortman, J. P. Brutman, C. J. Cramer, M. A. Hillmyer, W. R. Dichtel, Mechanically activated, catalyst-free polyhydroxyurethane vitrimers. *J. Am. Chem. Soc.* **137**, 14019–14022 (2015). doi:10.1021/jacs.5b08084 Medline

8. Y. Yang, Z. Pei, Z. Li, Y. Wei, Y. Ji, Making and remaking dynamic 3D structures by shining light on flat liquid crystalline vitrimer films without a mold. *J. Am. Chem. Soc.* **138**, 2118–2121 (2016). doi:10.1021/jacs.5b12531 Medline

9. Z. Pei, Y. Yang, Q. Chen, Y. Wei, Y. Ji, Regional shape control of strategically assembled multishape memory vitrimers. *Adv. Mater.* **28**, 156–160 (2016). doi:10.1002/adma.201503789 Medline

10. N. Zheng, Z. Fang, W. Zou, Q. Zhao, T. Xie, Thermoset shape-memory polyurethane with intrinsic plasticity enabled by transcarbamoylation. *Angew. Chem. Int. Ed. Engl.* **55**, 11421–11425 (2016). doi:10.1002/anie.201602847 Medline

11. M. Capelot, D. Montarnal, F. Tournilhac, L. Leibler, Metal-catalyzed transesterification for healing and assembling of thermosets. *J. Am. Chem. Soc.* **134**, 7664–7667 (2012). doi:10.1021/ja302894k Medline

12. Y. Yang, Z. Pei, X. Zhang, L. Tao, Y. Wei, Y. Ji, Carbon nanotube-vitrimer composite for facile and efficient photo-welding of epoxy. *Chem. Sci. (Camb.)* **5**, 3486–3492 (2014). doi:10.1039/C4SC00543K

13. Q. Chen, X. Yu, Z. Pei, Y. Yang, Y. Wei, Y. Ji, Multi-stimuli responsive and multi-functional oligoaniline-modified vitrimers. *Chem. Sci. (Camb.)* **8**, 724–733 (2017). doi:10.1039/C6SC02855A

14. E. Chabert, J. Vial, J.-P. Cauchois, M. Mihaluta, F. Tournilhac, Multiple welding of long fiber epoxy vitrimer composites. *Soft Matter* **12**, 4838–4845 (2016). doi:10.1039/C6SM00257A Medline

15. Z. Pei, Y. Yang, Q. Chen, E. M. Terentjev, Y. Wei, Y. Ji, Mouldable liquid-crystalline elastomer actuators with exchangeable covalent bonds. *Nat. Mater.* **13**, 36–41 (2014). doi:10.1038/nmat3812 Medline

16. S. J. Rowan, S. J. Cantrill, G. R. L. Cousins, J. K. M. Sanders, J. F. Stoddart, Dynamic covalent chemistry. *Angew. Chem. Int. Ed. Engl.* **41**, 898–952 (2002). doi:10.1002/1521-3773(20020315)41:6<898:AID-ANIE898>3.0.CO;2-E Medline

17. C. D. Roy, H. C. Brown, A comparative study of the relative stability of representative chiral and achiral boronic esters employing transesterification. *Monatsh. Chem.* **138**, 879–887 (2007). doi:10.1007/s00706-007-0699-x

18. O. R. Cromwell, J. Chung, Z. Guan, Malleable and self-healing covalent polymer networks through tunable dynamic boronic ester bonds. *J. Am. Chem. Soc.* **137**, 6492–6495 (2015). doi:10.1021/jacs.5b03551 Medline

19. J. J. Cash, T. Kubo, A. P. Bapat, B. S. Sumerlin, Room-temperature self-healing polymers based on dynamic-covalent boronic esters. *Macromolecules* **48**, 2098–2106 (2015). doi:10.1021/acs.macromol.5b00210

20. Y.-X. Lu, F. Tournilhac, L. Leibler, Z. Guan, Making insoluble polymer networks malleable via olefin metathesis. *J. Am. Chem. Soc.* **134**, 8424–8427 (2012). doi:10.1021/ja303356z Medline

21. P. Taynton, K. Yu, R. K. Shoemaker, Y. Jin, H. J. Qi, W. Zhang, Heat- or water-driven malleability in a highly recyclable covalent network polymer. *Adv. Mater.* **26**, 3938–3942 (2014). doi:10.1002/adma.201400317 Medline

22. M. Pepels, I. Filot, B. Klumperman, H. Goossens, Self-healing systems based on disulfide–thiol exchange reactions. *Polym. Chem.* **4**, 4955–4965 (2013). doi:10.1039/c3py00087g

23. T. F. Scott, A. D. Schneider, W. D. Cook, C. N. Bowman, Photoinduced plasticity in cross-linked polymers. *Science* **308**, 1615–1617 (2005). doi:10.1126/science.1110505 Medline

24. R. Nicolaÿ, J. Kamada, A. Van Wassen, K. Matyjaszewski, Responsive gels based on a dynamic covalent trithiocarbonate crosslinker. *Macromolecules* **43**, 4355–4361 (2010). doi:10.1021/ma100378r

25. M. M. Obadia, B. P. Mudraboyina, A. Serghei, D. Montarnal, E. Drockenmuller, Reprocessing and recycling of highly cross-linked ion-conducting networks through transalkylation exchanges of C–N bonds. *J. Am. Chem. Soc.* **137**, 6078–6083 (2015). doi:10.1021/jacs.5b02653 Medline

26. P. J. Flory, *Principles of Polymer Chemistry* (Cornell Univ. Press, 1953).

27. D. G. Hall, *Boronic Acids: Preparation, Applications in Organic Synthesis and Medicine* (Wiley-VCH, 2005).

28. R. Martin, S. L. Buchwald, Palladium-catalyzed Suzuki-Miyaura cross-coupling reactions employing dialkylbiaryl phosphine ligands. *Acc. Chem. Res.* **41**, 1461–1473 (2008). doi:10.1021/ar800036s Medline

29. R. P. Kambour, A review of crazing and fracture in thermoplastics. *J. Polymer Sci. Macromol. Rev.* **7**, 1–154 (1973). doi:10.1002/pol.1973.230070101

30. Y. Xu, C. M. Thurber, T. P. Lodge, M. A. Hillmyer, Synthesis and Remarkable Efficacy of Model Polyethylene-graft-poly(methyl methacrylate) Copolymers as Compatibilizers in

Polyethylene / Poly(methyl methacrylate) Blends. *Macromolecules* **45**, 9604–9610 (2012). doi:10.1021/ma302187b

31. D. B. Williams, M. Lawton, Drying of organic solvents: Quantitative evaluation of the efficiency of several desiccants. *J. Org. Chem.* **75**, 8351–8354 (2010). doi:10.1021/jo101589h Medline

32. G. Springsteen, B. Wang, A detailed examination of boronic acid-diol complexation. *Tetrahedron* **58**, 5291–5300 (2002). doi:10.1016/S0040-4020(02)00489-1

33. C. D. Roy, H. C. Brown, Stability of boronic esters—Structural effects on the relative rates of transesterification of 2-(phenyl)-1,3,2-dioxaborolane. *J. Organomet. Chem.* **692**, 784–790 (2007). doi:10.1016/j.jorganchem.2006.10.013

34. C. D. Roy, H. C. Brown, A study of transesterification of chiral (-)-pinanediol methylboronic ester with various structurally modified diols. *Monatsh. Chem.* **138**, 747–753 (2007). doi:10.1007/s00706-007-0681-7

35. J. W. B. Fyfe, E. Valverde, C. P. Seath, A. R. Kennedy, J. M. Redmond, N. A. Anderson, A. J. B. Watson, Speciation control during Suzuki-Miyaura cross-coupling of haloaryl and haloalkenyl MIDA boronic esters. *Chemistry* **21**, 8951–8964 (2015). doi:10.1002/chem.201500970 Medline

36. J. Yan, G. Springsteen, S. Deeter, B. Wang, The relationship among pKa, pH, and binding constants in the interactions between boronic acids and diols—It is not as simple as it appears. *Tetrahedron* **60**, 11205–11209 (2004). doi:10.1016/j.tet.2004.08.051

37. S. D. Bull, M. G. Davidson, J. M. H. van den Elsen, J. S. Fossey, A. T. A. Jenkins, Y.-B. Jiang, Y. Kubo, F. Marken, K. Sakurai, J. Zhao, T. D. James, Exploiting the reversible covalent bonding of boronic acids: Recognition, sensing, and assembly. *Acc. Chem. Res.* **46**, 312–326 (2013). doi:10.1021/ar300130w Medline

38. A. R. Goldberg, B. H. Northrop, Spectroscopic and computational investigations of the thermodynamics of boronate ester and diazaborole self-assembly. *J. Org. Chem.* **81**, 969–980 (2016). doi:10.1021/acs.joc.5b02548 Medline

39. G. De Bo, Combining mobile and dynamic bonds for rapid and efficient self-healing materials. *Chem* **1**, 668–673 (2016).

40. S. Yu, R. Zhang, Q. Wu, T. Chen, P. Sun, Bio-inspired high-performance and recyclable cross-linked polymers. *Adv. Mater.* **25**, 4912–4917 (2013). doi:10.1002/adma.201301513 Medline

41. B. Wunderlich, Ed., *Crystal Structure, Morphology, Defects, Macromolecular Physics*, vol. 1 (Academic Press, 1973).

42. K. Kendall, J. Crack propagation in lap shear joints. *Phys. D Appl. Phys.* **8**, 512–522 (1975). doi:10.1088/0022-3727/8/5/010

43. D. Maugis, Ed., *Adhesion and Rupture of Elastic Solids, Springer Series in Solid-State Sciences*, vol. 130 (Springer, 2000).